International Journal of Nanomedicine

Dovepress
Taylor & Francis Group

Open Access Full Text Article

ORIGINAL RESEARCH

Itraconazole-Loaded Polycaprolactone Nanoparticle Gel for Enhanced Transdermal Delivery: Development, Characterization, and ex vivo Evaluation

Sajjad Hussain[1,2], Nadia Shamshad Malik[1], Ume Ruqia Tulain[3], Alia Erum[3], Arshad Mahmood[4,5], Sohail Akram[1], Alina Javaid[1], Asmaa Jabeen[1], Chuxiao Shao[6], Shuanghu Wang[6], Ayesha Younas[6]

[1]Faculty of Pharmacy, Capital University of Science and Technology, Islamabad, Pakistan; [2]Amson Vaccines & Pharma, Islamabad, Pakistan; [3]College of Pharmacy, University of Sargodha, Sargodha, Pakistan; [4]Faculty of Pharmacy, Al Ain University, Abu Dhabi Campus, Abu Dhabi, United Arab Emirates; [5]AAU Health and Biomedical Research Center (HBRC), Al Ain University, Abu Dhabi, United Arab Emirates; [6]Central Laboratory of The Lishui Hospital of Wenzhou Medical University, The First Affiliated Hospital of Lishui University, Lishui People's Hospital, Lishui, Zhejiang, 323000, People's Republic of China

Correspondence: Nadia Shamshad Malik, Faculty of Pharmacy, Capital University of Science and Technology, Islamabad, Pakistan, Tel +923216802340, Email nadia.malik@cust.edu.pk; Ayesha Younas, Central Laboratory of The Lishui Hospital of Wenzhou Medical University, The First Affiliated Hospital of Lishui University, Lishui People's Hospital, Lishui, Zhejiang, 323000, People's Republic of China, Tel +86-13007613318, Email ay.ayeshayounas@gmail.com

Objective: Itraconazole (ITZ) is a BCS class II antifungal agent difficult to formulate due to its poor water solubility (<0.2 mmol /mL) and variable oral bioavailability (~55%). This study aimed to develop Polycaprolactone (PCL) nanoparticles to improve their transdermal delivery.

Methods: The nanoparticles were prepared using a modified nanoprecipitation method, resulting in ten formulations (F1 to F10). The optimized formulation (F2) was incorporated into a carbopol gel. Characterization included particle size, polydispersity index (PDI), zeta potential, encapsulation efficiency (EE), and in vitro drug release at pH 5.5 and 7.4. Ex vivo permeation, skin irritation, and stability were also evaluated.

Results: Formulation F2 (40 mg PCL, 2% Poloxamer 407 showed optimal properties: particle size of 154.6 nm, PDI (0.378), zeta potential (−10.7 ± 5.36 mV), and EE (88.4 ± 1.2%). A pH-dependent sustained release was observed, with 80.41% and 94.34% cumulative release at pH 5.5 and 7.4 over 24 hours, respectively, following Higuchi kinetics (R^2= 0.9804 at pH 5.5). The gel demonstrated significantly higher permeation (Q_{24}: 173.29 ± 3.12 μg/cm^2; Jss: 7.22 ± 0.15 μg/cm^2/h) versus plain gel (Q_{24}: 75.35 ± 1.35 μg/cm^2; Jss: 3.11 ± 0.08 μg/cm^2/h), with an enhancement ratio of 2.32. Characterization confirmed the amorphous state of ITZ and absence of interactions. The formulation was non-irritating (PII=0) and stable for three months.

Conclusion: A promising and biocompatible PCL-based gel was successfully developed, providing an effective approach for enhanced transdermal delivery of ITZ through sustained drug release and improved skin permeability.

Keywords: itraconazole, polycaprolactone, nanoparticles, transdermal delivery, pH- responsive release, BCS class II, skin permeation

Introduction

Fungal infections continue to represent a major global health burden, affecting more than one billion people every year. These infections contribute to over 1.5 million deaths worldwide. Among these, invasive fungal infections, mainly caused by Candida, Aspergillus, and Cryptococcus species, account for approximately 80% of mortality due to fungal diseases.[1] The economic consequences are similarly serious, with annual global antifungal treatment costs exceeding $7 billion due to the increased number of hospitalizations, the growing resistance to antifungal treatments, and the limited effectiveness of existing treatments.[2] Among the current antifungal agents, ITZ is a potent, broad-spectrum triazole. Its clinical use is limited due to poor water solubility (<0.2 μg/mL), high variability of oral bioavailability (~55%), and

Received: 14 August 2025
Accepted: 21 November 2025
Published: 24 December 2025

extensive plasma protein binding (~96%). As a Class II drug, ITZ is characterised by low solubility but high permeability, resulting in a limited absorption rate and unpredictable therapeutic results.[3] In addition, ITZ shows a limited dermal permeability, which makes topical or transdermal administration difficult.[4] Conventional formulation strategies, including cyclodextrin complexes, lipid emulsions, and solid dispersions, have achieved little improvement in bioavailability, often without addressing the need for sustained release, improved skin permeability, and reduced toxicity.[5] While cyclodextrins, for instance, improve aqueous solubility by encapsulating lipophilic drugs, this approach often leads to rapid release upon dilution, offering limited control over release kinetics and failing to create a sustained depot effect at the application site.[6]

To address these limitations, nanoparticles have emerged as a powerful tool. We selected polycaprolactone (PCL) as the polymeric matrix based on a strategic fit with ITZ's high lipophilicity (log P ~5.66). The hydrophobic core of PCL provides a thermodynamically compatible microenvironment for ITZ, facilitating high-affinity partitioning and enabling high encapsulation efficiency. This synergy not only ensures efficient drug loading but also underpins a sustained release profile, as drug diffusion through the PCL matrix is a rate-limiting step that prevents burst release.[7]

A key innovative aspect of our system is its pH-dependent design. The skin's surface maintains a characteristic acidic pH (typically 4.5–5.5), which can influence drug release kinetics. Our formulation is engineered to provide optimal release in this acidic microenvironment, facilitating drug penetration through the skin for systemic absorption. Importantly, the observed pH-dependent behaviour is not an intrinsic property of the PCL polymer but an emergent, formulation-engineered phenomenon. It arises from the synergistic interplay between the Poloxamer 407 stabilizer, which undergoes pH-dependent conformational changes at the nanoparticle interface, and the weak base characteristics of ITZ. This designed responsiveness ensures controlled drug release is optimized for the skin's acidic surface pH.

This represents a distinct advantage over cyclodextrin-based systems, as our PCL-based nanoparticles provide a dual function: enhancing apparent solubility through nanonization while acting as a sustained-release reservoir. Furthermore, PCL offers excellent biocompatibility, FDA-approved status, and slow degradation, which aligns with the goal of durable release to minimise systemic toxicity. PCL nanoparticles also protect the drug from premature degradation.[6]

For further optimisation of nanoparticle performance, Poloxamer 407 is used as stabilizer. Poloxamer 407 is a non-ionic tribolymer of PEO (PEO-PPO-PEO) with amphiphilic properties, which improves the dispersibility and stability of hydrophobic drugs in water. Its surface-active nature helps to stabilize nanoparticles, prevent aggregation and improve dissolution of the drug.[8] In addition, Poloxamer 407 inhibits efflux transporters such as P-glycoprotein, which may increase the uptake of the encapsulated drug into the skin and cells.[9] When Poloxamer 407 is used in combination with PCL, it forms a synergic delivery platform. PCL provides structural integrity and durability, while Poloxamer 407 improves permeability and bioavailability.[10] To achieve effective dermal application and a sustained therapeutic effect, the nanoparticles developed are formulated in a carbopol-based hydrogel suitable for transdermal drug delivery. This route bypasses hepatic first-pass metabolism, increases local drug concentrations and decreases systemic adverse reactions. Carbopol, a widely used synthetic polymer, has high viscosity, excellent bioavailability and enhanced permeability to the skin, making it the ideal vehicle for transdermal drug delivery.[11] This study, therefore, aims to develop a rationalised, nanotechnology-enabled transdermal delivery system for ITZ by the formulation of nanoparticles of PCL-Poloxamer incorporated in a carbopol gel matrix. The formulation is systematically assessed for its physicochemical properties, in vitro release kinetics and skin permeability. This integrated approach should address the main bottlenecks in the delivery of ITZ by increasing the solubility, stability, bioavailability and local efficacy of the drug, and ultimately provide a versatile platform that could be extended to other hydrophobic antifungal agents.

Materials and Methods

Materials

USP-grade ITZ was generously provided by Vision Pharma (Islamabad, Pakistan). Poloxamer 407 (a purified non-ionic surfactant) was obtained from Sigma-Aldrich (CHEMEI GmbH, Germany), Polycaprolactone (average Mn ~14,000 g/mol) was procured from Macklin Biochemical Co., Ltd. (CH1002, China), and carbopol® 934 was sourced from Spectrum Chemical Mfg. Corp. (USA), Dimethyl sulfoxide (DMSO), eucalyptus oil, and triethanolamine (TEA,

≥99%, analytical grade) were purchased from BioShop Canada Inc. Methanol, disodium hydrogen phosphate, sodium chloride, and glycerin (≥99%, USP grade) were supplied by Merck, Freshly distilled water was prepared in-house at the Faculty of Pharmacy, Capital University of Science and Technology (CUST), Islamabad.

Method

The nanoparticles were prepared using an optimized modified nanoprecipitation with control of critical process parameters, as shown in Figure 1. For the organic phase preparation, PCL was initially dissolved in DMSO under magnetic stirring at 500 rpm and 25°C. Complete polymer dissolution was achieved through bath sonication at 30°C for 15 minutes. For drug-loaded formulations, 10 mg of ITZ was gradually added to the PCL solution with continuous stirring at 800 rpm and maintained at 35°C for 15 minutes. The aqueous phase was prepared by dissolving Poloxamer 407 (2% w/v) in distilled water. Nanoparticle synthesis was performed by injecting the organic phase into the aqueous phase using a 22G needle at 0.25 mL/min.

ITZ solution was added dropwise (approximately 1 mL/min) under continuous stirring at 1000 rpm. This controlled rate is essential for two key reasons: It governs the nucleation and growth kinetics during nanoparticle formation, directly influencing the particle size and PDI. Moreover, it ensures a gradual integration of the drug into the polymeric matrix, which is fundamental for achieving high Encapsulation Efficiency (EE) by minimizing the rapid precipitation of free drug.[12]

The injection process was conducted under constant homogenization at 2000 rpm using an overhead homogenizer. For the complete separation of the free drug from the nanoparticle composition, the centrifugation was performed in the SCI-24 Scilifex centrifuge at 2,000 g for 60 minutes at 25 degrees Celsius. These parameters have been carefully optimized to ensure quantitative sedimentation of the nanoparticles without compromising their robustness.

The pellet was washed twice with 5 mL cold distilled water, followed by 1 minute of bath sonication. The purified nanoparticles were frozen at −20°C for 8 hours before lyophilization in a freeze dryer. The lyophilization protocol consisted of primary drying at −40°C and 0.1 mbar for 12 hours, followed by secondary drying at 25°C and 0.01 mbar for

Figure 1 Schematic Diagram of the Nanoprecipitation Method for ITZ-PCL Nanoparticle Preparation.

https://doi.org/10.2147/IJN.S560741

Table 1 Composition of Itraconazole-Loaded PCL Nanoparticle Formulations

Formulation	ITZ (mg)	Polymer PCL (mg)	Solvent DMSO (mL)	Poloxamer 407 (%)	Aqueous Phase Volume (mL)
F1	10	20	10	2.0	10
F2	10	40	10	2.0	10
F3	10	60	10	2.0	10
F4	10	80	10	2.0	10
F5	10	20	10	1.0	10
F6	10	20	10	3.0	10
F7	10	20	10	5.0	10
F8	10	20	10	2.0	20
F9	10	20	10	2.0	30
F10	10	20	10	2.0	40

an additional 12 hours.[13,14] Different formulations were prepared by varying the quantity of Polymer, surfactant, and volume of aqueous phase as given in Table 1.

The gel matrix was prepared using a controlled hydration method to ensure optimal polymer dispersion. Carbopol 934 (1% w/v) was gradually sprinkled into ice-cold distilled water under constant stirring at 2000 rpm using an overhead stirrer. The acidic polymer dispersion was then neutralized using triethanolamine (TEA, 0.5% v/v) added dropwise (0.1 mL/min) from a calibrated burette while monitoring pH with a calibrated pH meter.[15] The neutralization process continued until reaching the target pH range of 5.5–6.0, which is compatible with the skin. Following neutralization, the gel was subjected to a maturation period of 24 hours at 4°C to achieve complete polymer swelling and uniform viscosity. Eucalyptus oil was then incorporated as a permeation enhancer. The lyophilized ITZ-loaded PCL nanoparticles were redispersed in glycerin (5% v/v) using bath sonication until achieving a homogeneous suspension. This nanoparticle-glycerin premix was then slowly incorporated into the gel base at a rate of 0.5 mL/min using a syringe while maintaining gentle magnetic stirring (300 rpm) at 25±0.5°C. The mixing continued for an additional 30 minutes after complete addition to ensure uniform nanoparticle distribution without aggregation.[16]

Characterization

Encapsulation Efficiency Determination

The encapsulation efficiency of ITZ-loaded nanoparticles was determined by indirect quantification. After nanoparticle preparation, the dispersion was centrifuged at 2000×g for 60 minutes at 25 °C (Thermo Scientific, USA) to sediment the polymeric nanoparticles and to separate the free (unencapsulated) drug present in the aqueous supernatant. The clear supernatant was carefully withdrawn and analyzed spectrophotometrically using a UV–Visible spectrophotometer (Shimadzu UV-1800, Japan) at a λmax of 262 nm, which corresponds to the maximum absorbance of ITZ in the selected solvent system.[17] The method was previously reported and validated in literature.[18] The encapsulation efficiency was then calculated using equation 1:

$$Encapsulation\ Efficiency\ (\%EE) = \left(\frac{\mathrm{W}\ total\ -\ W\ free}{W\ total}\right) * 100 \quad (1)$$

Where:

W*total* = Total amount of drug initially added during nanoparticle formulation

W*free* = Amount of free (unencapsulated) drug found in the supernatant after centrifugation

In Vitro Drug Release Study

The in vitro release behaviour of nanoparticles loaded with ITZ was assessed using a USP Type II (paddle) dissolution apparatus under controlled sink conditions. For the simulation of the sustained release environment, nanoparticles were encapsulated in pre-soaked dialysis membrane bags (MWCO 12–14 kDa) that allowed for selective drug diffusion and retained nanoparticles. Dissolution studies have been performed in two media, phosphate buffer (pH 7.4) and acetate

buffer (pH 5.5). In order to improve the solubility of ITZ due to its poor water solubility profile, sodium lauryl sulphate (SLS) 0.5% w/v was added to each buffer.[19] For physiological simulation, the volume of buffer solution in each vessel was kept at 500 mL, and the rotating paddle was set at 100 rpm to ensure uniform mixing. At predetermined time intervals (0.5, 1, 2, 3, 4, 6, 8, 12, 18, and 24 hours), 2 mL samples were withdrawn and replaced immediately with equal volumes of fresh preheated medium to maintain both constant volume and sink conditions. The withdrawn aliquots were filtered through membrane filters at a pressure of 0.45 mmol membrane filter to remove any particulate matter and residues from the membrane. The concentration of ITZ in each sample was measured using a UV spectrophotometer at 262 nm using a standard calibration curve.[20] The cumulative percentage of drug release was calculated and plotted as a function of time. Dissolution data were fitted into various mathematical models, including zero-order, first-order, Higuchi, and Korsmeyer-Peppas models. The best fit was determined by comparing the correlation coefficients (R^2) of each of the two models, while the release exponent (n) of the Korsmeyer-Peppas equation provided an insight into the mechanism of drug release, distinguishing between Fickian diffusion, anomalous transport, or case-II relaxation. All measurements were performed in triplicate, and the results were expressed as mean ± standard deviation to ensure statistical robustness.[21]

Swelling Behavior

The swelling behaviour of ITZ-loaded PCL-Poloxamer 407nanoparticles was assessed to evaluate their ability to absorb fluid and their potential impact on the drug release kinetics. Accurately weighed dried nanoparticle samples (~20 mg) were immersed in phosphate-buffered saline (PBS) at pH 7.4 and pH 5.5 to simulate physiological and skin surface conditions, respectively. Samples were incubated at 37 ± 0.5 °C under mild agitation. At predefined time intervals (1, 3, 6, 12, and 24 hours), the swollen nanoparticles were gently removed, surface moisture was blotted using filter paper to remove excess buffer, and the samples were reweighed. All measurements were performed in triplicate.[22,23]

The swelling capacity (%) was calculated using the following equation 2

$$Swelling\ Capaciy(\%) = \frac{W2 - W1}{W1} X100 \tag{2}$$

Where:

W_1 = Initial dry weight of nanoparticles

W_2 = Weight of swollen nanoparticles after excess buffer removal

Determination of Particle Size and Poly Dispersity Index (PDI)

The particle size (Z-average) and the PI (polydispersity index) of the ITZ-NP were determined by dynamic light scattering (DLS) using the Zetasizer Nano ZS (Malvern Instruments, UK). The samples were diluted 1:20 (v and v) with 2% (w/v) of Poloxamer 407 solution. The measurements were made at 25°C with a backscatter detection angle of 173°, and each sample was analysed in three steps.[24]

Surface Morphology

The morphological properties of ITZ-NP have been assessed by using field-emission scanning electron microscopy (FE-SEM; JSM-7900F, JEOL Ltd., Japan). A 10 µL aliquot of nanoparticle suspension was deposited on aluminium foil, air-dried at 25 ± 2°C, and mounted on aluminium strata by a conductive carbon fibre tape. The samples were sputtered with a 3nm gold-palladium thickened veil to increase the conductivity. The imaging was carried out at a voltage of 5–10 kV and a working distance of 5–10 mm.[25]

Thermo Gravimetric Analysis (TGA) and Differential Scanning Calorimetry (DSC)

The thermal behaviour of lyophilized ITZ-NPs was investigated using simultaneous differential scanning Calorimetry thermogravimetric analysis (DSC-TGA; SDT Q600, TA Instruments). Approximately 5–10 mg of sample was sealed in aluminium crucibles and heated from 25°C to 300°C at 10°C/min under nitrogen purge (50 mL/min). Thermal events (glass transition Tg, melting Tm, decomposition) were analyzed using TA Universal Analysis software.[26]

Fourier-Transform Infrared Spectroscopy (FTIR)

The molecular interactions between ITZ and the polymer compounds were evaluated by the FTIR (Spectrum Two, PerkinElmer) in the range of 4000–400 cm^{-1}. The samples were prepared as potassium bromide (KBr) pellets (1:100 sample: KBr) and scanned with a resolution of 4 cm^{-1} with 32 accumulations. The background correction was made using pure KBr. Characteristic functional group vibrations were compared between pure components and nanoparticles to determine potential drug-polymer interactions.[27]

X-Ray Diffraction (XRD)

Crystallinity of ITZ in nanoparticle formulation was assessed with a Cu-Kα irradiation source (λ = 1.5406, 40 kV, 30 mA) using an X-ray Diffractometer (Scintag XGEN-4000, Advanced Diffraction System, Scintag Inc., USA). Samples were placed in a zero-background silicon holder and scanned over a 2θ range of 4–50° at a scan rate of 2°/min with a step size of 0.02°. Diffraction patterns were collected in continuous scan mode and analyzed using Scintag DataScan (v4.0) software.[28]

Physical Parameters of Prepared Formulations Gel

The optimized nanoparticle formulation has been incorporated in a gel matrix of Carbopol 934 (1.0% w/w) to enhance topical delivery of the drug. The resulting formulations have been rigorously assessed for critical quality characteristics by means of a comprehensive physical characterization. The Formulations were visually checked for colour, clarity, and homogeneity and phase separation under ambient conditions. The pH of the surface was determined in three times by calibration calibrated digital pH meter (PHS-25CW, BANTE Instruments, China) at 25 ± 1 °C. Before measurements, the instrument was standardized with buffer solutions of pH 4.0, 7.0, and 10.0. The electrode was allowed to be equilibrated with the sample for 30 seconds before recording to ensure accuracy and reproducibility.

The dynamic viscosity of the pharmaceutical formulae was precisely determined in centipoise (Cp) by using a Brookfield DV2T viscometer with spindle S64. All measurements were performed at 25 ± 0.5 degrees Celsius to ensure consistency and reliability of the rheological data, which are critical to correlate the properties of the formulation with the diffusion behaviour. Flow-through curves were analyzed to determine the viscosity profiles and to evaluate the pseudoplastic behaviour to ensure reproducibility and consistency between the lots. Approximately 350 mg of gel was placed in the centre of the glass plate (10 x 5 cm), and a second glass plate of the same size and weight (5.8 ± 0.1 g) was dropped freely from a height of 5 cm. After 1 minute, the average diameter of the diffusion surface was measured in centimetre.[29]

Ex vivo Skin Permeation Studies

To assess the transdermal potential of the optimized nanoparticle formulation, ex vivo permeation studies were conducted using Franz-diffusion cells and excised intra-abdominal skin from healthy New Zealand white rabbits. Two gel formulations were evaluated: F2 Gel: ITZ -loaded PCL nanoparticle incorporated gel, Plain Gel: Gel containing free ITZ. Full-thickness rabbit skin was excised, cleaned to remove subcutaneous fat, and equilibrated in phosphate-buffered saline (PBS, pH 7.4) for 1 hour. The skin samples were then stored at −20 °C and melted down before use.[30] Each skin sample was inserted between the donor and receptor compartments of the Franz diffusion cell (diffusion area = 2.54 cm^2) so that the stratum corneum is parallel to the donor side. The receptor compartment was filled with 20 mL of PBS (pH 5.5, to mimic skin surface conditions), maintained at 37 ± 0.5 °C, and stirred continuously with a magnetic stirrer at a speed of 600 rpm. An accurately weighed amount (1 g) of either F2 gel or plain gel was applied uniformly to the donor compartment. At specific intervals (0.5, 1, 2, 6, 8, 12, and 24 h), 2 mL samples were taken from the receptor compartment and replaced by the same volume of fresh PBS to ensure that the saturation conditions were maintained. The amount of the drug per square meter (μg/cm^2) was plotted against the time elapsed to obtain a permeability profile.[31] From the linear portion of the curve (steady state), the steady-state flux (Jss) was calculated from equation 3:

$$Jss = \frac{\Delta Q}{A\Delta t} \tag{3}$$

ΔQ = amount of drug permeated during steady state (μg)

A = effective diffusion area (2.54 cm^2)

Δt = time interval during steady-state linear region (h)

To compare permeation enhancement, the Enhancement Ratio (ER) was calculated from equation 4

$$ER = \frac{Jss\,(F2gel)}{Jss\,(Plaingel)} \tag{4}$$

All experiments were conducted in triplicate (n = 3). Data are expressed as mean ± standard deviation (SD). An unpaired two-tailed Student's *t*-test was used to determine statistical significance, with $p < 0.05$ considered significant.

Skin Irritation Test

The dermal biocompatibility of the ITZ-loaded gel was evaluated in vivo using healthy adult New Zealand white rabbits (Oryctolagus cuniculus, n=9) in accordance with OECD Guideline 404.[32] The study protocol was approved by the Research Ethics Committee of the Faculty of Pharmacy, Capital University of Science and Technology, Islamabad (Approval No. REC/FoP/F2024/02). All animals were acclimatized under standard laboratory conditions and were blindly randomized to treatment groups. The housing, handling, and experimental procedures strictly adhered to institutional ethical standards and the internationally recognized Guide for the Care and Use of Laboratory Animals to ensure animal welfare throughout the study.[33]

Animals were randomly divided into three groups (n = 3 per group):

- Test group: ITZ- nanoparticle-loaded gel
- Positive control: 0.8% w/v sodium lauryl sulfate (SLS) solution
- Negative control: Untreated site (baseline skin response)

All animals were kept in a controlled environment (22 ± 2 °C, 55 ± 5% RH, 12 h light/dark cycle) with unrestricted access to standard food and water for 48 hours. Before the experiment, the dorsal surface was carefully shaved with an electric clipper 24 hours before administration to avoid microscopic damage. To preserve the biochemical and barrier integrity of the skin tissue, a standardized protocol was followed. Excised rabbit skin was rinsed with normal saline, carefully trimmed of subcutaneous fat and connective tissue, and equilibrated in phosphate-buffered saline (PBS, pH 7.4) for 1 hour prior to mounting in the diffusion cells. For storage, the prepared skin was wrapped in aluminum foil and stored at –20 °C, with each sample being thawed at room temperature before the experiment to maintain a consistent and functional barrier for permeation studies.[34]

Approximately 6 cm^2 test area was demarcated on each rabbit. Each sample (0.1 g) was applied to the designated area using a sterile polypropylene spatula under an occlusive patch. Observations were made during the initial 4 hours and at 24 h, 48 h, and 72 h post-application for signs of erythema, edema.

The Draize scoring system was used to quantify the severity of erythema and edema:

- 0 = None
- 1 = Mild (faint or light pink coloration, <1/3 area)
- 2 = Moderate (definite erythema, 1/3–2/3 area)
- 3 = Severe (dark red, >2/3 area or spreading beyond site)

The Primary Irritation Index (PII) was calculated after 72 hours using the Equation 5

$$PII = (Sum\ of\ erythema + edema\ scores)/(number\ of\ animals\ X\ No.\ of\ readings) \tag{5}$$

Based on OECD classification, PII < 0.5 is considered non-irritant.[35]

Stability Study

The physical stability of the selected gel formulations has been assessed under standardized storage conditions following the ICH guidelines. The samples were packed in light-resistant containers (glass bottles with aluminium foil lining) and stored under three different environmental conditions: 4 ± 1°C (refrigerated), 25 ± 2°C (ambient), and 40 ± 2°C/75 ± 5%

RH (accelerated), respectively. The acceptance criteria for physical stability included maintaining a homogenous appearance, viscosity at a level of at least 10%, and pH stability (calibration of pH by a calibrated pH meter) at predetermined intervals (0, 1, 2, and 3 months). Formulations were evaluated for:

1. Visual characteristics (color, homogeneity, phase separation)
2. pH stability (using calibrated pH meter)
3. Rheological properties (viscosity measurements at controlled shear rates)

The acceptance criteria for physical stability included maintenance of homogeneous appearance, viscosity within ±10% of initial values, and pH stability within ±0.5 units.[36]

Statistical Analysis

All data were analysed using SPSS Statistics 26.0 (IBM, USA). One-way analysis of variance (ANOVA) with Tukey's post-hoc test was applied to compare means. A p-value < 0.05 was considered statistically significant. Results are presented as mean ± SD (n = 3).

Results and Discussions

Encapsulation Efficiency (EE)

The encapsulation efficiency of ITZ-loaded PCL nanoparticles varied significantly across the prepared formulations, with values ranging from 70.2% to 88.4% ($p < 0.05$) as shown in Table 2 Among these, formulation F2 exhibited the highest EE of 88.4 ± 1.2%, which was statistically superior to the other formulations, as confirmed by one-way ANOVA followed by Tukey's post-hoc test ($p < 0.05$). In the polymer content group (F1 to F4), increasing PCL concentration from 20 mg to 40 mg significantly improved EE from 78.2% to 88.4% ($p < 0.05$). However, further increases in PCL content to 60 mg (F3, 81.5 ± 1.4%) and 80 mg (F4, 80.1 ± 1.5%) resulted in a decline in EE compared to F2, with differences being statistically significant ($p < 0.05$), suggesting the existence of an optimal polymer concentration beyond which no additional encapsulation advantage is achieved.[37] In the surfactant concentration group (F5 to F7), EE was significantly affected by Poloxamer 407 content. A lower surfactant concentration (1%, F5) resulted in a reduced EE of 72.6 ± 1.9%, which was significantly lower than F2 ($p < 0.05$). Increasing Poloxamer 407 concentration to 3% (F6, 80.9 ± 1.3%) and 5% (F7, 79.8 ± 1.6%) improved EE compared to F5 but failed to reach the performance of F2, with statistical differences remaining significant ($p < 0.05$).[38] These findings indicate that 2% Poloxamer 407 represents an optimal concentration for achieving high encapsulation, likely due to an ideal balance between nanoparticle stabilization and prevention of drug leakage. Among Formulations, F8 to F10, an inverse relationship between aqueous volume and EE was evident. Increasing the aqueous phase from 10 mL (F2, 88.4 ± 1.2%) to 20 mL (F8, 76.8 ± 1.5%), 30 mL (F9, 74.5 ± 1.7%), and 40 mL (F10, 70.2 ± 2.0%) resulted in a statistically significant decrease in EE ($p < 0.05$), likely due to enhanced drug

Table 2 Encapsulation Efficiency (%EE) of ITZ-Loaded PCL Nanoparticle Formulations (N = 3)

Formulations	Encapsulation Efficiency (% EE)
F1	78.2 ± 1.6
F2	88.4 ± 1.2
F3	81.5 ± 1.4
F4	80.1 ± 1.5
F5	72.6 ± 1.9
F6	80.9 ± 1.3
F7	79.8 ± 1.6
F8	76.8 ± 1.5
F9	74.5 ± 1.7
F10	70.2 ± 2.0

diffusion into the aqueous phase during nanoparticle formation.[39] These systematic trends collectively demonstrate that formulation F2, containing 40 mg PCL, 2% Poloxamer 407, and 10mL aqueous phase, achieved the most favourable encapsulation efficiency, offering a statistically optimized system for effective ITZ encapsulation and stable nanoparticle formation.[40]

The observed trends can be mechanistically explained as follows. Increasing the concentration of PCL initially improves EE (F1 to F2) by increasing the availability of polymer chains for drug uptake.[41] However, excessive polymer content (F3 to F4) increases the viscosity of the solution, which prevents efficient nanoparticle formation and promotes drug diffusion into the water, thereby reducing EE.[42] Similarly, variations in Poloxamer 407 concentration demonstrated a dual role: at optimal levels (2%, F2), the surfactant reduced interfacial tension and stabilized nanoparticles,[43] resulting in high encapsulation. At higher levels (3–5%, F6–F7), excessive micelle formation may have caused partial drug partitioning into the aqueous phase, lowering EE.[44] The volume of the aqueous phase also has a negative effect on the EE, as larger volumes (F8-F10) dilute the organic phase more rapidly, leading to a decreased encapsulation.[45]

The non-linear relationship between PCL concentration and EE is a well-documented phenomenon in nanoprecipitation systems, arising from the interplay between thermodynamic affinity and kinetic process dynamics. The initial increase in EE with polymer concentration (20–40 mg PCL) results from enhanced hydrophobic interactions, where a greater polymer mass provides a more compatible microenvironment for lipophilic ITZ molecules, promoting efficient drug partitioning and entrapment within the polymer matrix during rapid nanoparticle formation.[41] However, beyond the optimal concentration (40 mg PCL in this study), a further increase in polymer content leads to a marked rise in the viscosity of the organic phase, which adversely affects two key kinetic steps: (i) diffusion of the organic phase into the aqueous medium, and (ii) efficient droplet breakup during homogenization. The resulting impaired mixing and slower solvent displacement cause premature drug precipitation outside the polymeric network, thereby lowering EE.[42] This non-linear trend reflects the balance between drug–polymer affinity and diffusion-controlled kinetics intrinsic to nanoprecipitation.

In vitro Drug Release and Kinetics

The drug release behaviour of ITZ-loaded PCL nanoparticles was systematically investigated under simulated skin surface (pH 5.5) and physiological (pH 7.4) conditions to elucidate the predominant release mechanisms and identify the most promising formulation. The cumulative drug release profiles for all formulations (F1–F9) are depicted in Figure 2, while corresponding release kinetic parameters derived from zero-order, first-order, Higuchi, and Korsmeyer–Peppas models are summarized in Table 3. At pH 5.5, representing the mildly acidic environment of human skin, all formulations exhibited a sustained and controlled drug release profile over 24 hours. The predicted cumulative drug release at the end of 24 hours ranged from 62.0% ± 2.5% to 82.0% ± 3.2%, with statistically significant differences among the formulations ($p < 0.05$, one-way ANOVA followed by Tukey's post-hoc test). Notably, Formulation F2 exhibited the most favorable release profile, achieving the highest cumulative drug release of 82.0% ± 3.2%, which was significantly greater ($p < 0.05$) than all other tested formulations. Additionally, F2 demonstrated the strongest correlation with the Higuchi model ($R^2 = 0.9804$), confirming a robust diffusion-controlled release mechanism. These results indicate that F2 is the optimal formulation for achieving efficient drug release on the skin surface. Other formulations, including F3 (74.0% ± 2.8%), F5 (75.0% ± 3.1%), and F8 (73.0% ± 2.6%), showed moderate release profiles, while formulations F1, F4, F7, and F9 exhibited comparatively lower cumulative drug release (62.0% to 70.0%) with no statistically significant differences within this group ($p > 0.05$). Kinetic modelling confirmed that the Higuchi model, which describes diffusion-controlled drug release from a homogenous polymeric matrix, provided the best overall fit for most formulations at pH 5.5. Specifically, eight out of nine formulations exhibited strong linearity with R^2 values exceeding 0.91, indicating that Fickian diffusion was the dominant release mechanism under these conditions. The superior fit of F2 further supports its favourable release behaviour and suggests effective diffusion of ITZ from the nanoparticulate matrix. These findings align with previous studies demonstrating diffusion-dominated release from hydrophobic polymer matrices under mildly acidic, non-swelling conditions.[46,47] The in-vitro release study demonstrated a cumulative drug release of 94.34% of F2 at pH 7.4 over 24 hours. The in-vitro release at pH 7.4 reached approximately 50% within 10 hours, followed by gradual release up to 80% by 24 hours. Formulations F2 and F3 showed the highest release rates, nearing 80% cumulative

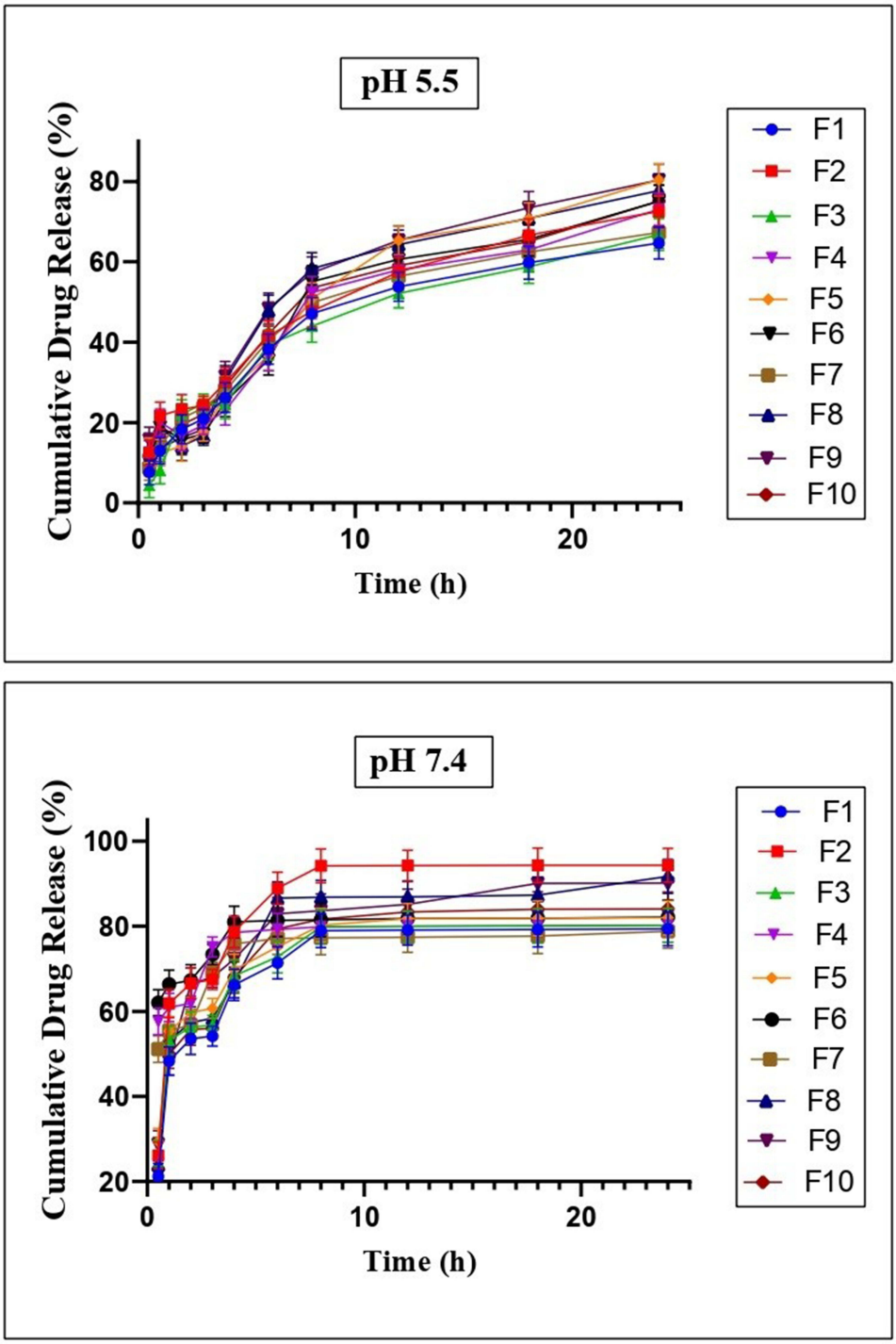

Figure 2 In vitro, drug release kinetics of ITZ loaded PCL nanoparticles (F1-F10) in simulated skin pH 5.5 and at physiological pH 7.4.

release. In contrast, F6-F9 exhibited slower release, plateauing around 60%. This pH-dependent pattern suggests polymer swelling enhances drug diffusion under physiological conditions. Overall, the fit to the Higuchi model decreased for several formulations, with R^2 values falling below 0.70 for F4 (R^2 = 0.6268), F6 (R^2 = 0.6679), and F7 (R^2 = 0.6685), suggesting that additional mechanisms such as matrix swelling, relaxation, or erosion contribute to drug release under alkaline conditions, beyond pure diffusion.[48] At this pH, the Korsmeyer–Peppas model provided improved statistical performance, indicating a transition to anomalous (non-Fickian) release behaviour. For instance, F9 exhibited

Table 3 In vitro Drug Release Kinetic Models (Zero-Order, First-Order, Higuchi, Korsmeyer–Peppas) of ITZ Loaded PCL Nanoparticles (F1-F10) at pH 5.5 and 7.4

Sample	pH	Zero Order		First Order		Higuchi		Korsmeyer-Peppas R^2			Weibull Model	
		R^2	K	R^2	K	R^2	K	R^2	K	n	R^2	K
F1	5.5	0.8691	4.2187	0.429	0.2987	0.9653	14.045	0.9318	21.7158	0.2683	0.746	0.1385
	7.4	0.5154	8.7142	0.1822	0.3937	0.7125	29.483	0.721	67.2749	0.0043	0.5939	0.0515
F2	5.5	0.9206	4.4980	0.3817	0.3279	0.9804	16.450	0.969	22.1322	0.3307	0.8461	0.0827
	7.4	0.4853	10.6768	0.1689	0.4140	0.672	36.169	0.6998	82.1200	0.0011	0.5827	0.0420
F3	5.5	0.8682	4.2490	0.4358	0.2738	0.9681	13.842	0.9484	17.6730	0.3690	0.6398	0.1977
	7.4	0.5173	8.2470	0.1716	0.3994	0.7052	30.690	0.7171	69.1319	0.0046	0.6024	0.0419
F4	5.5	0.8929	4.0769	0.4386	0.3190	0.9389	14.964	0.9192	19.2977	0.3594	0.7892	0.0790
	7.4	0.3835	2.9964	0.1381	0.4093	0.6268	34.032	0.6345	74.5645	0.0040	0.3673	0.0335
F5	5.5	0.9165	3.4815	0.5198	0.3007	0.9565	14.791	0.9466	23.9848	0.2602	0.7846	0.1542
	7.4	0.5088	8.0624	0.1659	0.4022	0.7049	31.795	0.769	71.3336	0.0037	0.6241	0.0389
F6	5.5	0.8817	4.6930	0.4572	0.3195	0.936	14.994	0.9069	20.4550	0.3330	0.771	0.0947
	7.4	0.389	2.9276	0.1331	0.4147	0.6679	35.391	0.4575	76.4040	0.0073	0.4253	0.0259
F7	5.5	0.8645	4.3338	0.4081	0.3052	0.9643	15.053	0.9358	23.7079	0.2563	0.7436	0.1346
	7.4	0.4163	3.6864	0.1486	0.4033	0.6685	32.120	0.5874	67.8528	0.0305	0.4134	0.0414
F8	5.5	0.8432	4.5586	0.4461	0.3253	0.919	16.127	0.8359	24.4698	0.2810	0.6895	0.1103
	7.4	0.5623	9.2102	0.1902	0.4012	0.7396	32.354	0.7077	63.1798	0.0915	0.6115	0.0467
F9	5.5	0.8672	3.4428	0.4647	0.3102	0.9388	16.002	0.8666	23.6103	0.3002	0.7112	0.1573
	7.4	0.5485	7.7592	0.1783	0.3979	0.7358	33.152	0.8755	66.8136	0.0715	0.5595	0.0623
F10	5.5	0.8879	4.6638	0.4246	0.3150	0.9666	15.672	0.9282	19.8883	0.3696	0.7738	0.1230
	7.4	0.5359	8.8423	0.185	0.3970	0.7237	30.880	0.7057	69.8522	0.111	0.5863	0.0518

a significantly better fit to the Korsmeyer–Peppas model ($R^2 = 0.8755$) compared to the Higuchi model ($R^2 = 0.7358$, $p < 0.05$), while F5 showed a similar trend (Korsmeyer–Peppas $R^2 = 0.7690$, Higuchi $R^2 = 0.7049$). The corresponding n-values, all below 0.45, further confirm the involvement of complex release mechanisms, likely involving polymer relaxation and matrix erosion under physiological conditions.[49] Collectively, these findings demonstrate a statistically significant, pH-dependent release behaviour for ITZ-loaded nanoparticles. A Fickian, diffusion-dominated release profile was observed at pH 5.5, transitioning to anomalous, non-Fickian mechanisms at pH 7.4 ($p < 0.05$, based on comparative model fits and n-values). Among all tested formulations, F2 emerged as the most promising candidate for dermal drug delivery, offering the highest drug release efficiency coupled with a robust diffusion-controlled release mechanism at the skin surface.[50]

Furthermore, the distinct pH-dependent release—with significantly higher release at physiological pH (7.4)—suggests that the formulation can respond to the physiological environment, potentially offering enhanced release in the deeper skin layers. The synergy between the PCL matrix and the Poloxamer 407 stabilizer in F2 creates a "Goldilocks zone", where the formulation is neither too hydrophobic to limit release nor too hydrophilic to lose its sustained-release characteristic. This pH-dependent behaviour can be explained by a coordinated two-stage mechanism operating at the nanoparticle interfaces. The pH-dependent drug release observed in our system arises from a coordinated two-stage mechanism. At the nanoparticle interface, Poloxamer 407 undergoes pH-dependent conformational changes: at pH 7.4, hydrated PEO chains form a dense steric barrier limiting water diffusion, while at pH 5.5, mild acidity disrupts hydrogen bonding, partially dehydrating and coiling the chains to increase interfacial free volume and enhance water ingress. This is corroborated by higher swelling ratios for formulation F2 at pH 5.5 (1.42) versus pH 7.4 (1.39). Concurrently, enhanced water penetration plasticizes the PCL matrix, increasing chain mobility and reducing diffusional barriers. The weak base character of ITZ further enhances drug solubility under acidic conditions, strengthening the concentration gradient (ΔC) that drives diffusion. The excellent correlation with the Higuchi model ($R^2 = 0.9804$ at pH 5.5) confirms diffusion-controlled kinetics through this optimally hydrated polymeric network.

The drug release data were further analysed using the Weibull model to gain additional insights into the release mechanisms. The Weibull model is particularly useful for describing dissolution and release phenomena from complex systems, as it does not assume any specific drug release mechanism.[51] At pH 5.5, the Weibull model showed moderate correlation coefficients (R^2 = 0.64–0.85), with formulation F2 demonstrating the strongest fit (R^2 = 0.8461). The Weibull rate parameter (K) values ranged from 0.08 to 0.20 at pH 5.5, with lower K values generally corresponding to more sustained release profiles. At physiological pH (7.4), the Weibull model exhibited poorer correlation (R^2 = 0.37–0.62), suggesting that the release kinetics under these conditions may not be adequately described by this empirical model. The superior fit of the Higuchi model at skin pH (5.5), compared to the Weibull model, provides stronger evidence for a diffusion-controlled release mechanism in the acidic environment relevant for transdermal application.

Swelling Behaviour

The swelling dynamics of nanoparticles are of key importance in transdermal drug delivery systems, where controlled hydration controls the drug diffusion kinetics while preserving structural integrity at the skin interface. Moderate swelling at skin pH (~5.5) is necessary to increase the release of the drug by hydration-induced matrix relaxation without compromising the NP adhesion to the stratum corneum, a critical balance for a sustained transdermal delivery.[52] In this study, the pH-dependent swelling profiles were systematically assessed under physiological (pH 7.4) and simulated acidic (pH 5.5) conditions, as shown in Figure 3. A one-way ANOVA with Tukey's post-hoc tests (α = 0.05, n = 3) revealed a significant compositional effect on the equilibrium swelling ratios ($F(9, 40) = 28.6$, $p<0.001$), confirming that formulation design critically modifies hydration behaviour (Figure 3). The formulation F2 (40 mg PCL, 2% Poloxamer 407) demonstrated an optimal swelling ratio of 1.42± 0.05 at pH 5.5 and 1.39 ± 0.04 at pH 7.4, resulting in a balance between hydration-induced drug release and mechanical stability. This controlled swelling is in line with the ideal ranges reported for transdermal systems, where excessive hydration (>1.5) risks particle disintegration, while insufficient swelling (<1.3) limits the diffusion of the drug.[53] Increasing the concentration of the PCL from 20 mg (F1) to 40 mg (F2) considerably reduced the swelling by 6.4% ($p = 0.007$).

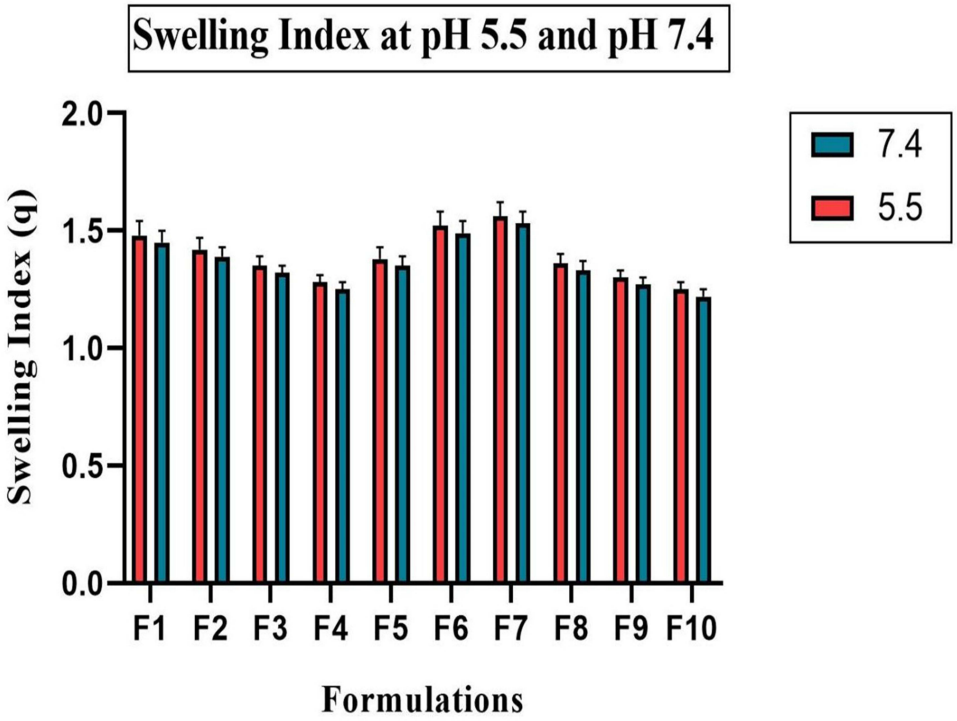

Figure 3 Swelling Index (q) of nanoparticle formulations (F1 to F10) at pH 5.5 and pH 7.4. Data are presented as mean ± SD (n = 3). Statistical significance was determined by one-way ANOVA with Tukey's post-hoc test (α = 0.05).

Conversely, preparations with a higher content of Poloxamer 407 (F7: 5% surfactant) showed destabilizing swellings (1.563 ± 0.061 at pH 5.5; p = 0.003 vs F2), consistent with surfactant-mediated micellization and pore formation. Increasing the aqueous phase volume from 10 mL (F2) to 40 mL (F10) reduced swelling ratios by 11.2% (1.248 ± 0.038; p < 0.001 vs F2), attributed to diminished polymer packing density during nanoprecipitation. Despite this, pH sensitivity (quantified as the % variation in swelling between pH 5.5 and 7.4) remained statistically constant across formulations (2.1%; p = 0.22–0.48), suggesting that surface hydrophilicity is primarily regulated by the protonation of terminal carboxyl groups of the PCL (pKa) and not by the bulk matrix.[54] Notably, acidic skin pH (5.5) in all NPs induced an increase in swelling higher than physiological pH (7.4) per protonation-induced hydrophilic enhancement. This pH response is beneficial to the transdermal system, as localized swelling at the skin surface may increase the rate of drug release at the application site. The robustness of the swelling profile of F2, combined with its pH tolerance, supports its selection as the preferred formulation for further characterization.

In particular, the concentration of PCL and the content of Poloxamer 407 have been identified as key determinants of the swelling behaviour, muco-adhesion strength and drug release kinetics. The moderate levels of both components (as optimized in formulation F2) allowed sufficient hydration and relaxation of the polymer chain, resulting in a balanced swelling and a strong adhesion to the skin. On the other hand, increased PCL content resulted in higher matrix density and decreased porosity, which prevented water uptake and slowed drug diffusion, whereas higher surfactant concentrations increased water uptake, but decreased the structural integrity of the gel, resulting in decreased adhesion and faster release. Together, these results indicate that a controlled extent of swelling is necessary to maintain mechanical stability, ensure strong adhesion, and facilitate diffusion-controlled release.

Particle Size, Polydispersity Index (PDI) and Zeta Potential

Particle size, PDI, and zeta potential were determined only for the optimized formulation (F2). Since the optimization process was based primarily on encapsulation efficiency and drug release characteristics across all batches (F1–F10), detailed physicochemical characterization was conducted on the best-performing formulation to represent the final optimized system. The particle size and surface characteristics of nanoparticles are critical determinants of their performance, particularly for transdermal and topical drug delivery applications. In this study, dynamic light scattering (DLS) analysis revealed that the ITZ-loaded PCL nanoparticles (Formulation F2) exhibited a Z-average hydrodynamic diameter of 154.6 nm with a dominant peak at 118.9 nm (Figure 4). Nanoparticles within the size range of 100–200 nm are considered optimal for topical delivery, as they facilitate enhanced penetration into the stratum corneum and effective distribution within the viable epidermis, while minimizing the likelihood of systemic absorption.[55] The PDI of the formulation was recorded as 0.378, indicating a moderately narrow size distribution. While a PDI value below 0.3 is indicative of monodisperse systems, values between 0.3 and 0.5 are generally acceptable for polymeric nanoparticle formulations, especially those prepared by nanoprecipitation using amphiphilic stabilizers such as Poloxamer 407.[56] The observed PDI reflects the controlled formulation parameters and efficient stabilization of nanoparticles, ensuring uniform particle size distribution, which is essential for consistent drug release and reproducible biological performance.

The electrokinetic stability of the nanoparticles was assessed by zeta potential analysis, which showed a value of −10.7 ± 5.36 mV. Although colloidal systems with zeta potential values exceeding ±30 mV are generally considered electrostatically stable, polymeric nanoparticle systems stabilized with non-ionic surfactants such as Poloxamer primarily rely on steric hindrance to prevent particle aggregation.[57] The slight negative surface charge observed in this study is attributed to the terminal carboxyl and ester functional groups present on the PCL chains, as well as the partial adsorption of the surfactant at the nanoparticle surface. This negative surface potential contributes to colloidal stability while minimizing the risk of aggregation during storage and application. Furthermore, nanoparticles with lower surface charge have been associated with reduced skin irritation potential, an essential attribute for transdermal and topical formulations.[58]

These results highlight that formulation F2, containing 40 mg PCL, 2% Poloxamer 407, and 10-mL aqueous phase, achieved an optimal balance of small particle size (154.6 nm), moderate PDI (0.378), and high EE (88.4%). The relatively low negative zeta potential (−10.7 mV) is consistent with steric stabilization by Poloxamer rather than electrostatic stabilization, minimizing aggregation while ensuring good dispersion stability.[59]

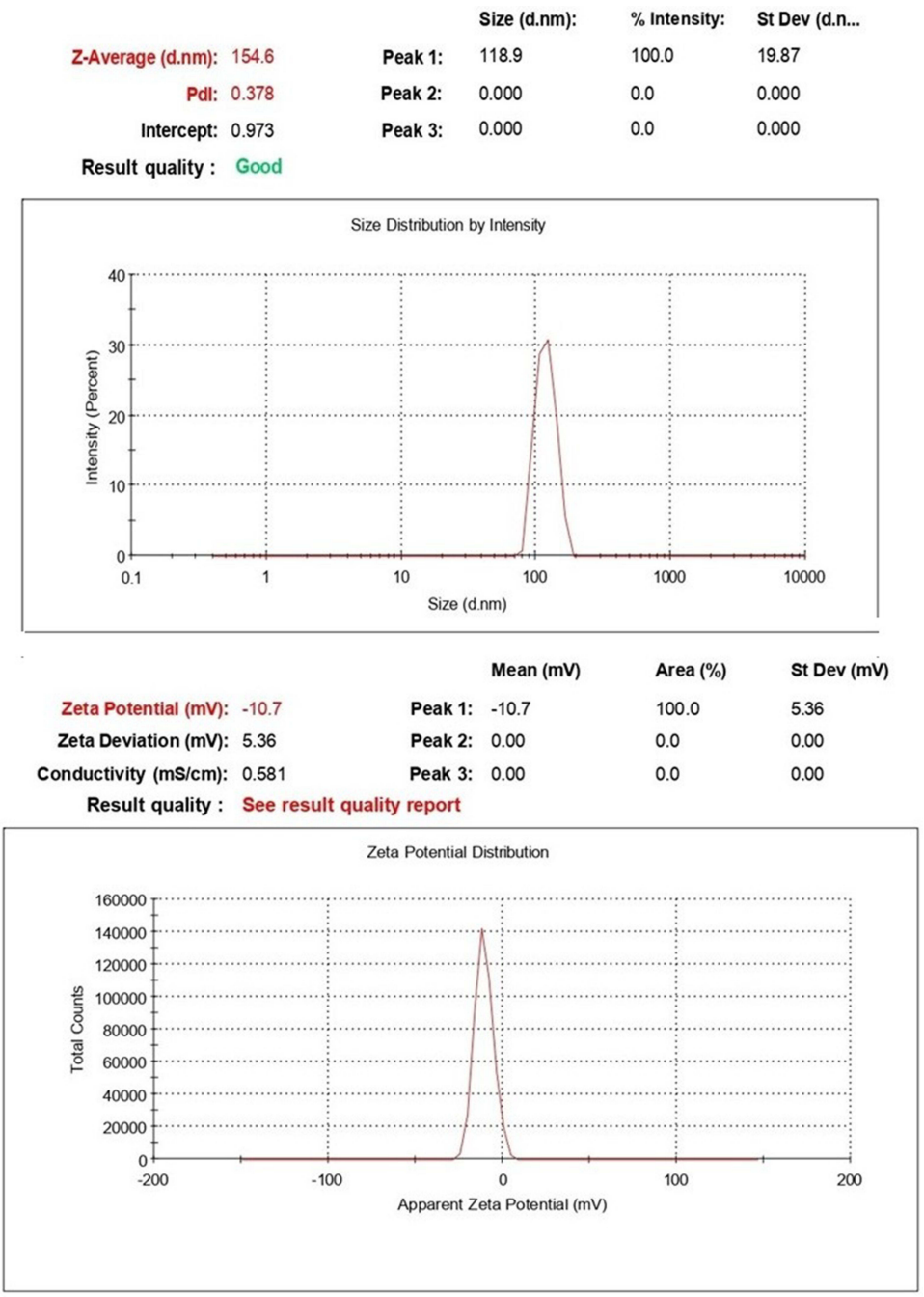

Figure 4 Hydrodynamic size and surface charge of ITZ-loaded PCL nanoparticles. The particle size distribution and zeta potential were measured by dynamic light scattering. The red text denotes the key reported values of Z-Average and Zeta Potential, confirming a nanometric formulation with moderate colloidal stability.

Scanning Electron Microscopy (SEM)

The surface morphology and structural characteristics of the developed PCL nanoparticles were investigated using Scanning Electron Microscopy, and the representative micrographs at different magnifications are presented in Figure 5. At lower magnifications (100× and 250×), the nanoparticles appeared as agglomerated particulate clusters, which may be attributed to the hydrophobic nature of PCL and the lyophilization process that promotes particle aggregation. Such agglomeration is frequently reported for polymeric nanoparticles owing to weak van der Waals interactions and the absence of stabilizing agents on the particle surface.[60] With progressive magnification (500× to 5000×), the micrographs revealed more detailed surface architecture of the nanoparticles. The nanoparticles exhibited a distinct, irregular, flake-

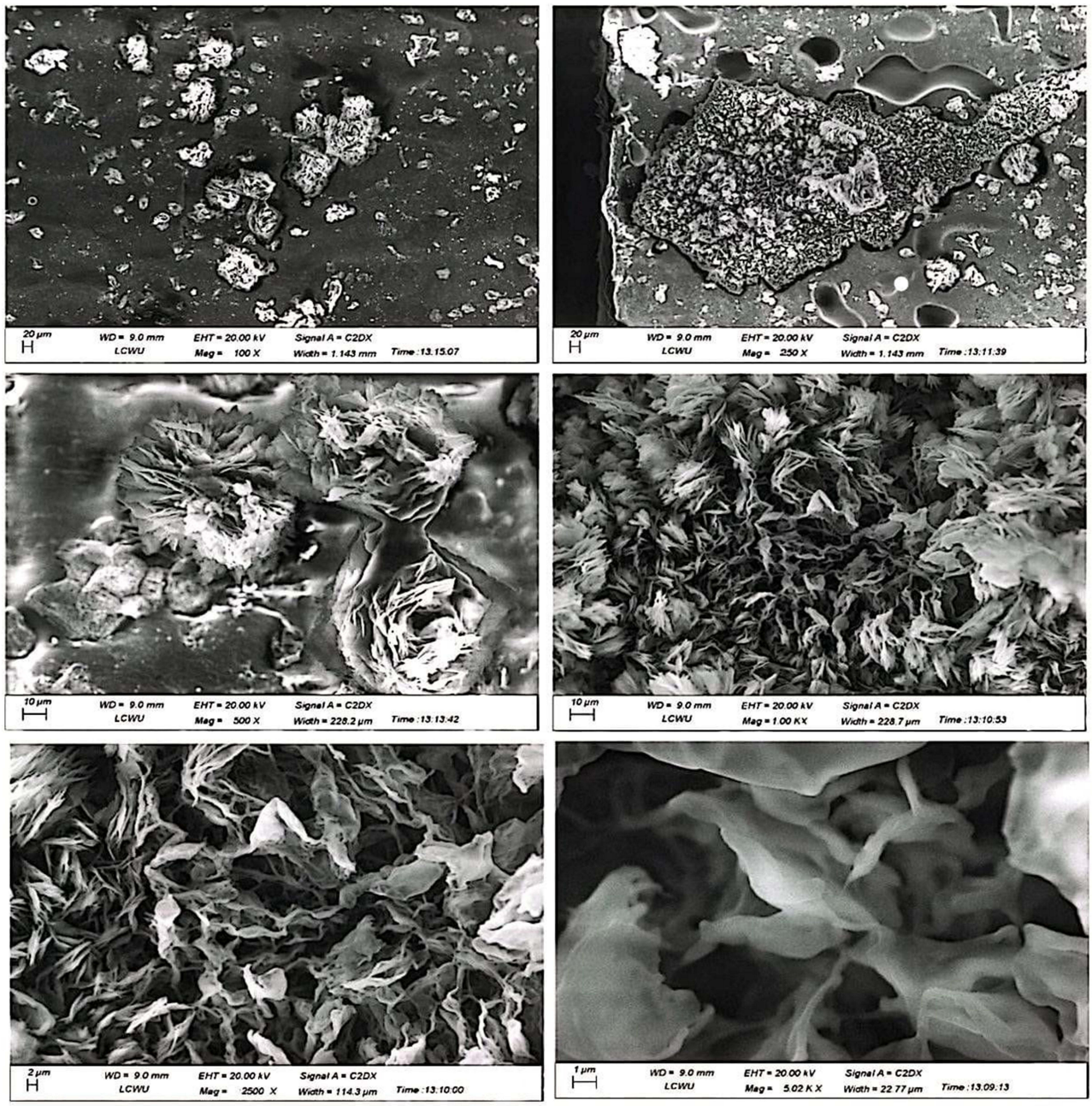

Figure 5 Scanning electron micrographs of ITZ-loaded PCL nanoparticles at various magnifications.

like morphology with interconnected porous structures and surface roughness. The porous appearance and wrinkled texture can be attributed to solvent evaporation and polymer precipitation during nanoparticle formation via the emulsification-solvent evaporation technique. Such morphological features are desirable for enhancing the effective surface area, which can facilitate higher drug loading and sustained release profiles. The pronounced porosity and interconnected voids observed at higher magnifications are indicative of the structural rearrangement of the PCL matrix during solvent removal. The presence of such porous networks is particularly advantageous for controlled drug delivery applications, as it can provide diffusion channels for drug molecules and contribute to prolonged release kinetics.[61] Furthermore, the irregular and rough surface morphology may enhance mucoadhesive or skin-interactive properties in topical or transdermal delivery applications, thereby improving drug permeation.[62] Overall, the SEM analysis confirmed

https://doi.org/10.2147/IJN.S560741

the successful fabrication of PCL nanoparticles with characteristic porous, rough, and irregular morphology, consistent with the design objectives for controlled and sustained drug delivery.

FTIR Analysis

FTIR spectroscopy was conducted to evaluate potential physicochemical interactions between ITZ, PCL, Poloxamer 407, and to confirm the successful incorporation of ITZ into the nanoparticle matrix (Figure 6). The FTIR spectrum of pure ITZ exhibited characteristic absorption bands at approximately 1700 cm^{-1} corresponding to carbonyl (C=O) stretching vibrations, and at 1515 cm^{-1}, attributed to C=C stretching within the aromatic rings.[63] The spectrum of PCL displayed a prominent ester carbonyl (C=O) stretching band at ~1720 cm^{-1} and methylene ($–CH_2$) stretching vibrations around 2940 cm^{-1}, confirming the presence of the aliphatic polyester backbone.[64]

Poloxamer 407 demonstrated its typical spectral features, with strong C–O–C stretching vibrations at approximately 1100 cm^{-1} and characteristic C–H stretching bands near 2880 cm^{-1}.[65] The FTIR spectrum of the ITZ-loaded PCL nanoparticle formulation retained all major characteristic peaks of ITZ, PCL, and POL, with minor shifts and peak broadening, particularly in the regions corresponding to C=O and C–O–C stretching vibrations. Notably, no new peaks or significant changes in the spectral profile were observed, indicating the absence of chemical interactions or covalent bond formation between the drug and the excipients.[66] These findings suggest that ITZ was physically encapsulated within the

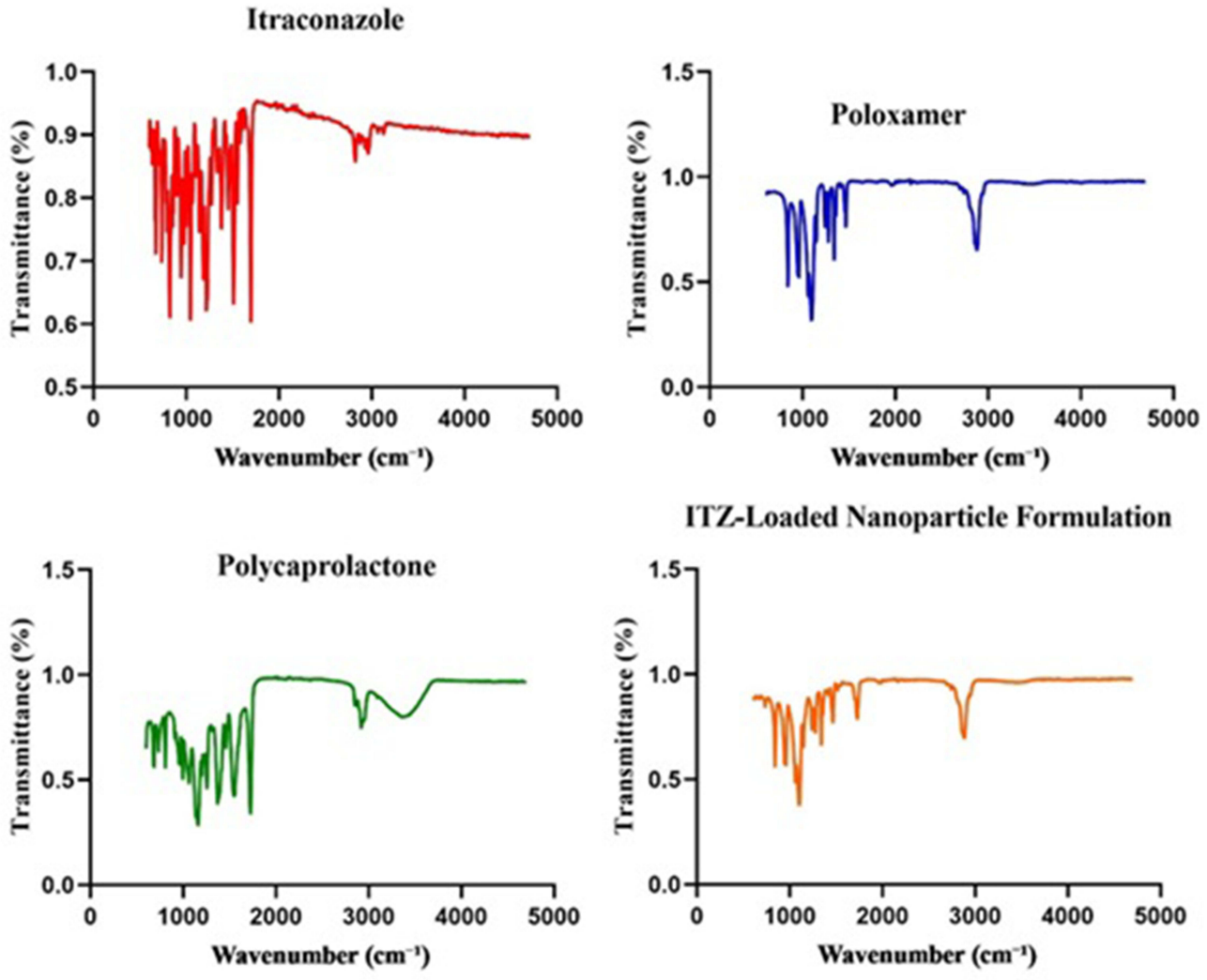

Figure 6 FTIR spectra of pure Itraconazole, polycaprolactone, Poloxamer 407, and ITZ-loaded nanoparticle formulation.

polymeric matrix without undergoing structural modification. The observed minor shifts and broadening are likely attributable to hydrogen bonding and weak physical interactions between the drug and polymer components, which are commonly reported in nanoparticulate systems.[67] The preservation of key functional groups and the absence of additional peaks confirm the chemical compatibility of the components and the successful entrapment of ITZ within the nanoparticle system.

X-Ray Diffraction Pattern (XRD)

The crystalline behaviour of pure components and the ITZ-loaded nanoparticle formulation was systematically evaluated using X-ray diffraction, with the diffraction patterns presented in Figure 7. Pure ITZ exhibited multiple sharp and intense diffraction peaks at 2θ values of approximately 12.5°, 15.8°, 17.3°, 19.5°, 21.7°, and 25.4°, confirming its highly crystalline nature.[28] These distinct peaks are characteristic of the ordered lattice structure of ITZ. In contrast, PCL displayed a broad, diffused halo centered around 20.2° 2θ, accompanied by a weak crystalline peak at approximately 23.5°, indicative of its semi-crystalline structure. This behaviour reflects the partial crystalline domains typical of PCL-based polymers. Similarly, the Poloxamer diffractogram revealed intense, sharp peaks located at 19.2°, 23.3°, 36.1°,

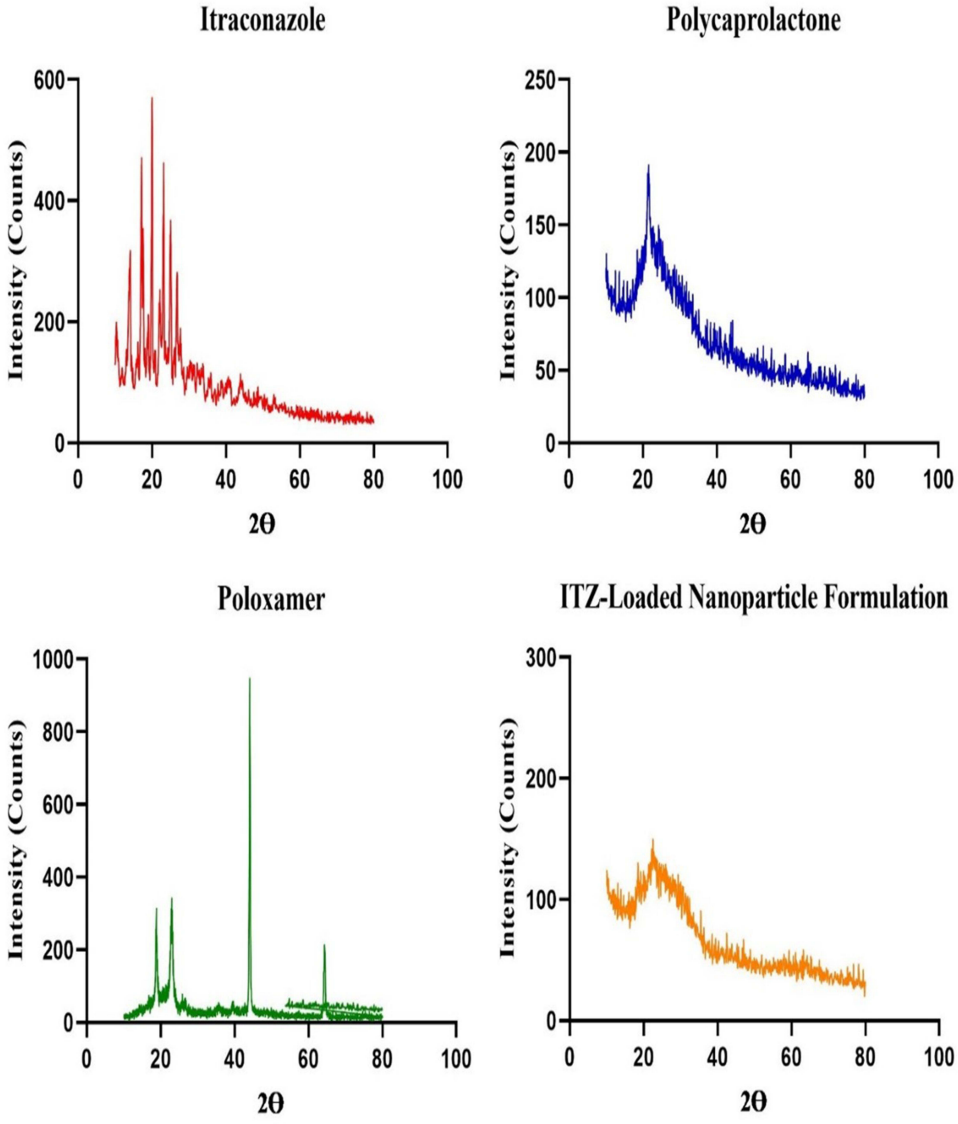

Figure 7 XRD Patterns of Pure Itraconazole, Polycaprolactone, Poloxamer 407 and ITZ-Loaded Nanoparticle Formulation.

https://doi.org/10.2147/IJN.S560741

42.5°, and 62.8°, confirming its crystalline nature, consistent with literature reports for Poloxamer 407. Remarkably, the ITZ-loaded nanoparticle formulation demonstrated a significant loss of the characteristic crystalline peaks of ITZ, exhibiting only a broad, amorphous halo between 15° and 35° 2θ, corresponding to the polymeric matrix. The complete disappearance of ITZ-specific peaks confirms successful molecular dispersion of the drug within the polymeric carrier system, resulting in amorphization. The absence of crystalline ITZ signals, coupled with the broad amorphous profile of the formulation, suggests effective drug-polymer interactions that inhibit drug recrystallization. This transformation from crystalline to amorphous state is particularly advantageous, as it is well-recognized to enhance drug solubility, dissolution rate, and ultimately, bioavailability.[68] These XRD findings substantiate the successful fabrication of a physically stable, amorphous ITZ-loaded nanoparticle system with promising potential for improving the oral bioavailability of poorly soluble drugs.

The observed disappearance of characteristic crystalline ITZ peaks in the XRD diffractogram of our formulations provides direct evidence of drug amorphization within the polymeric matrix.[69] This transformation is critically significant because the amorphous state possesses a higher Gibbs free energy than its crystalline counterpart. This elevated energy state directly translates to a lower thermodynamic barrier for dissolution. Consequently, this amorphization is the fundamental driver behind the enhanced apparent solubility and accelerated dissolution rate observed in our study.[70] The molecularly dispersed drug no longer requires energy to break down a stable crystal lattice, allowing for more rapid hydration and release. This rationale is firmly supported by established literature on solid dispersions.[71]

Differential Scanning Calorimetry (DSC) Analysis

Differential Scanning Calorimetry was conducted to evaluate the thermal behaviour and physical state of ITZ within the PCL–Poloxamer nanoparticle matrix as shown in Figure 8. The thermogram of pure ITZ exhibited a sharp endothermic peak at 167.44°C, corresponding to its melting point, which confirms its crystalline nature.[72] In contrast, this peak value in the thermogram of nanoparticles loaded with ITZ was absent or significantly decreased, suggesting that the drug is converted into an amorphous or molecularly dispersed state within the polymeric system. The PCL showed a melting point of around 59–61°C, which is in line with its semi-crystalline polyester structure, and this peak was maintained in the nanoparticle formulation, although with a reduced intensity, probably due to the plasticizing effect of Poloxamer 407.[73] Poloxamer showed two distinct endothermic peaks at 59.09 °C and 197.62 °**C** indicating the presence of an ordered crystalline structure. Blank nanoparticle formulation exhibited a broad and less intense thermal transition compared to excipients. The absence of a sharp ITZ peak in the formulation thermogram is a confirmation of successful encapsulation and indicates that the drug is not chemically involved but rather physically incorporated into the PCL matrix. The transition of ITZ from a crystalline to an amorphous state is particularly advantageous for enhancing the solubility and dissolution rate of poorly water-soluble drugs such as ITZ. These findings are consistent with previous reports in which the disappearance or enhancement of ITZ melting peaks in DSC thermogram was attributed as evidence of drug amorphization and uniform dispersion within nanoparticle carriers.[68]

Thermo-Gravimetric Analysis (TGA)

Thermogravimetric analysis was used to study the thermal degradation profiles of pure ITZ and ITZ-loaded PCL nanoparticles (Figure 9). The thermogram of pure ITZ revealed a sharp, single-step degradation event initiating at 369.37°C, consistent with its intrinsic decomposition behaviour.[74] The PCL degraded with significant mass losses between 250–350°C due to breakdown of its polymer backbone, whereas Poloxamer started degrading around 150°C, likely because of the breakdown of its PEO-PPO segments. The blank nanoparticle formulation showed a multi-phase degradation pattern comprising loss of moisture below 100°C and polymer decomposition in the range of 200–350°C; however, ITZ-loaded nanoparticles had a similar pattern to that of polymeric drug-delivery systems. This initial weight loss (5–8%) was due to evaporation of residual moisture. The primary degradation occurred between 250–380°C, corresponding to the thermal decomposition of the PCL polymer backbone and the encapsulated ITZ. The absence of a distinct ITZ degradation peak at 369.37°C in the nanoparticle formulation confirmed effective drug encapsulation within the polymeric matrix, with a concomitant shift in degradation onset temperatures. This observation implies greater thermal stabilization of ITZ due to molecular-level dispersion in the PCL nanoparticles, as reported earlier.[75]

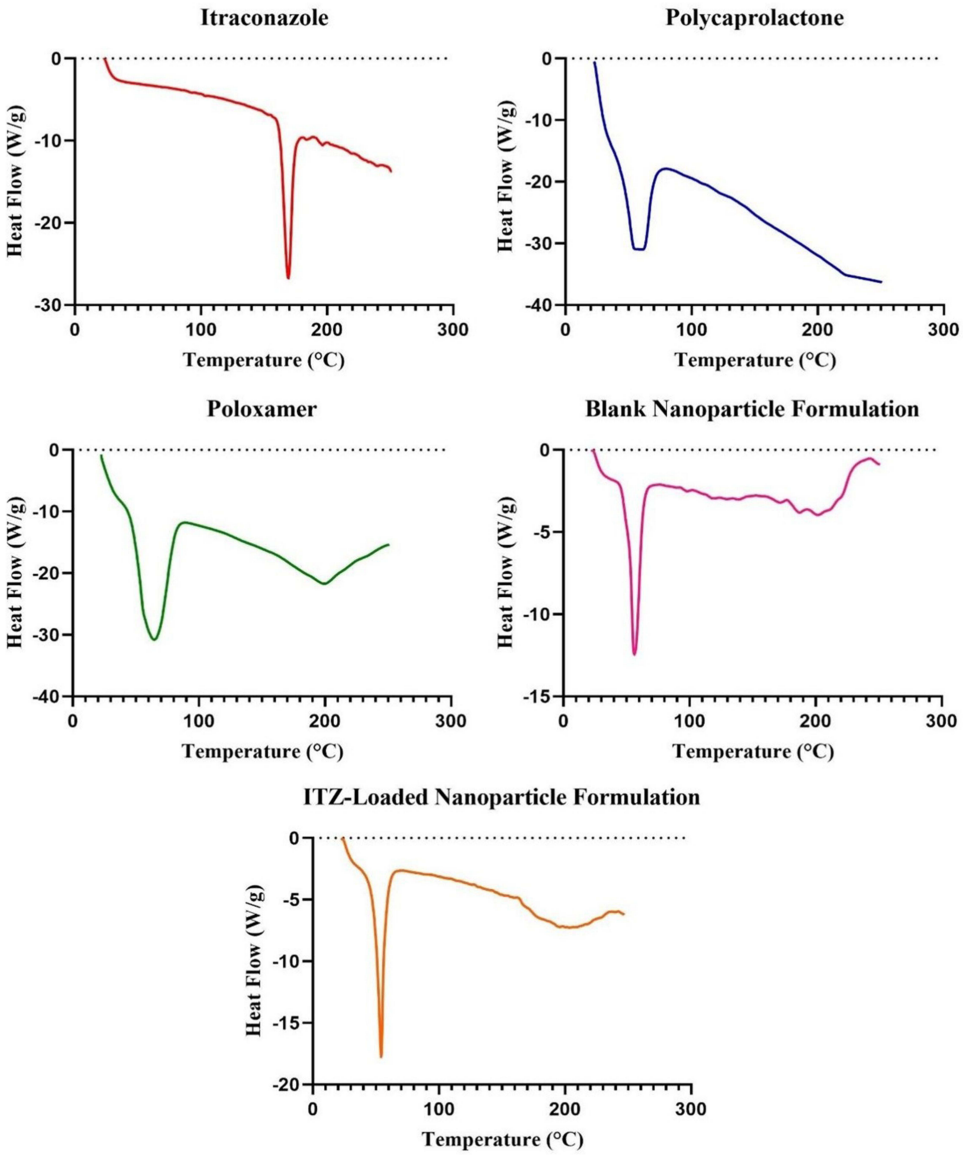

Figure 8 DSC thermogram of Pure Itraconazole, Polycaprolactone, Poloxamer 407, Blank Nanoparticle Formulation and ITZ-Loaded Nanoparticle Formulation.

Physical Evaluation of ITZ-Loaded Gel Formulation

The developed gel formulation containing ITZ-loaded PCL nanoparticles in a Carbopol 934 matrix has demonstrated promising pharmacological properties that are suitable for topical administration. The findings are summarized in Table 4. The gel was translucent and homogeneous, with no observable phase separation or grittiness, indicating effective nanoparticle dispersion and formulation stability. Compatibility with stratum corneum at pH 6.46 ± 0.01 and minimization of the risk of local irritation make it suitable for topical administration.[76,77] Rheological analysis revealed pseudoplastic (non-Newtonian) flow behaviour that is beneficial for topical formulations. Furthermore, the spreadability value of 6.08 ± 0.12 cm indicates sufficient flow characteristics, ensuring effortless application with minimal mechanical force. Overall, the results confirm the physical resistance, ease of use, and suitability of the formulation for effective local administration of ITZ. The nanoparticle gel demonstrated pseudoplastic (shear-thinning) characteristics and maintained this characteristic throughout storage, suggesting that the polymeric network remained structurally stable and no significant change in viscosity was observed, ensuring consistent spreadability and performance.

https://doi.org/10.2147/IJN.S560741

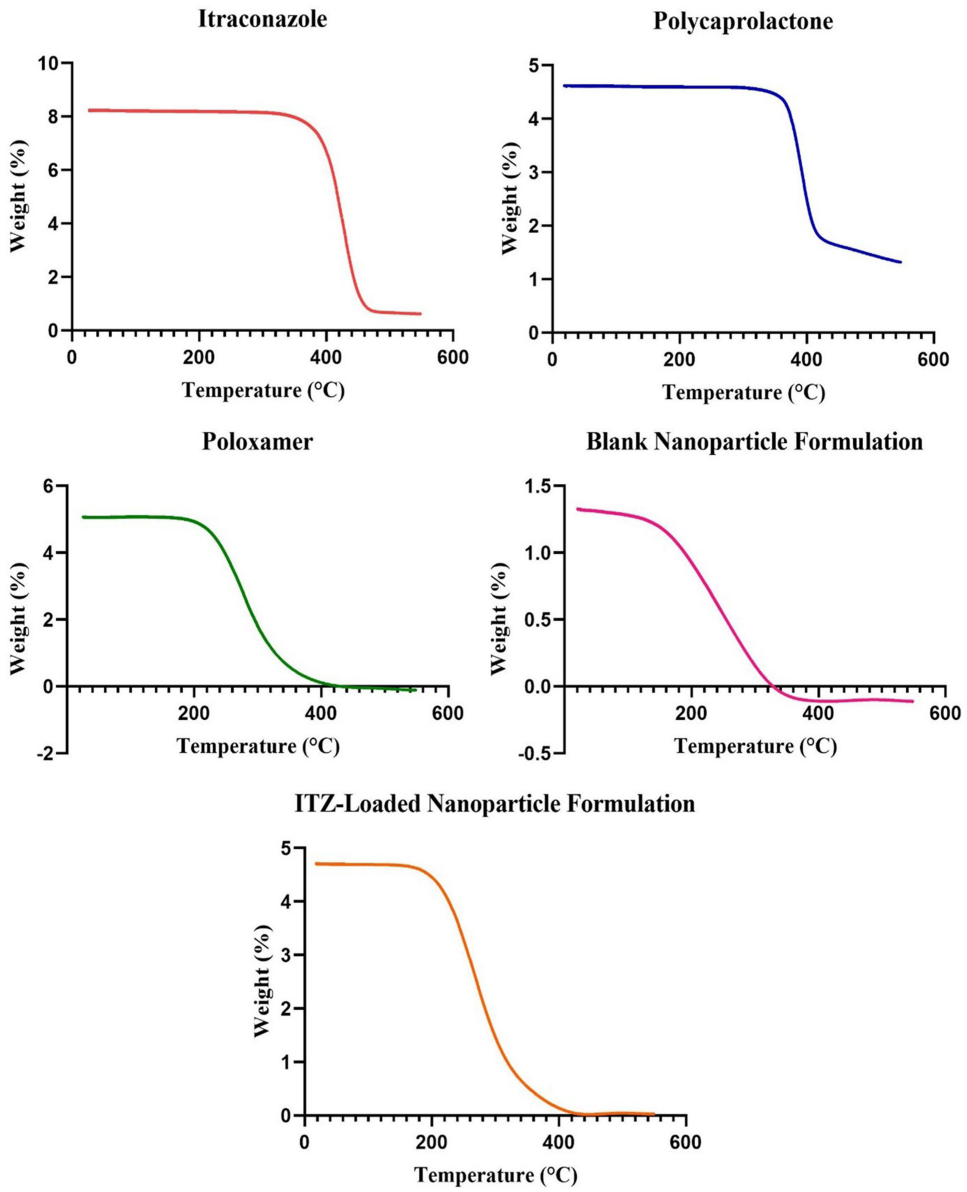

Figure 9 TGA thermogram of Pure Itraconazole, Polycaprolactone, Poloxamer 407, Blank Nanoparticle Formulation and ITZ-Loaded Nanoparticle Formulation.

Ex vivo Skin Permeation Study

Ex vivo skin permeation studies revealed significantly enhanced transdermal delivery of ITZ from the F2 nanoparticle-loaded gel compared to the plain ITZ gel. After 24 hours, the cumulative drug permeation (Q_{24}) from the F2 nanoparticle gel reached 173.29 ± 3.12 μg/cm^2, representing a 129.9% increase relative to the plain gel (75.35 ± 1.35 μg/cm^2) ($p <$

Table 4 Physicochemical and Rheological Evaluation of ITZ-Loaded Gel

Parameter	Result (Mean ± SD)	Interpretation
Appearance	Translucent, homogeneous gel	No phase separation or grittiness observed
pH	6.46 ± 0.01	Within physiological range, safe for dermal application
Viscosity (cP at 0.5 rpm)	13,360 ± 125	Suitable for topical use; shear-thinning behavior
Rheological behavior	Pseudoplastic (non-Newtonian)	Promote spreadability and retention on skin
Spreadability (cm)	6.08 ± 0.12	Ensures ease of application with minimal mechanical force

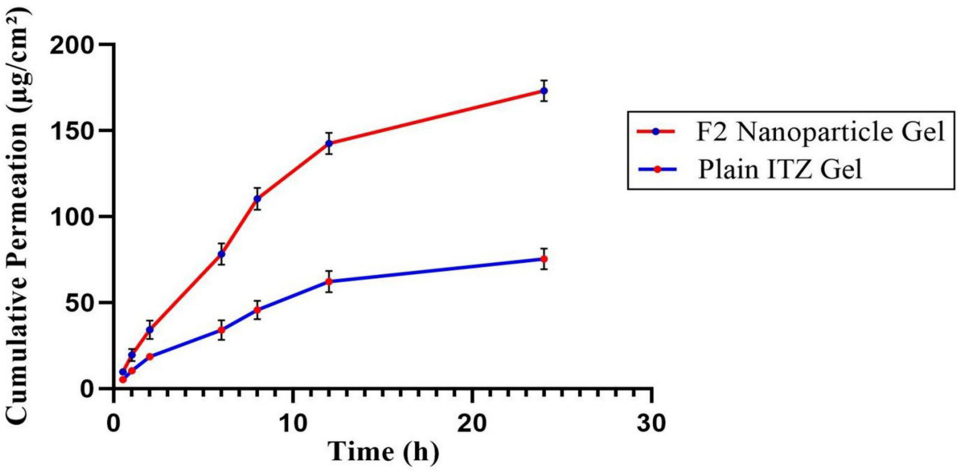

Figure 10 Cumulative permeation of ITZ from Plain ITZ Gel and F2 Nanoparticle Gel across excised rabbit skin (Mean ± SD, n = 3).

0.001), as illustrated in Figure 10. This remarkable improvement can be attributed to the nanometric particle size of the formulation, which enhances surface area and facilitates deeper penetration into the skin layers. Furthermore, the incorporation of Poloxamer 407, a well-established permeation enhancer, contributed to this effect by disrupting intercellular lipid bilayers and increasing skin hydration, thereby promoting drug transport across the stratum corneum.[78,79] The steady-state flux (Jss) of the F2 nanoparticle gel was also significantly higher (6.32 ± 0.15 µg/cm^2/h) compared to the plain gel (2.58 ± 0.08 µg/cm^2/h), corresponding to a 145% increase ($p < 0.001$), further confirming the superior permeation profile of the nanoparticle-based system (Table 5). Additionally, the calculated Enhancement Ratio (ER) for the F2 nanoparticle gel was 2.45, indicating a more than two-fold enhancement in permeation compared to the plain gel. The lag time (T_{lag}), representing the time required for drug molecules to establish steady-state diffusion across the skin barrier, was significantly reduced in the F2 nanoparticle gel (1.5–2.2 hours) compared to the conventional ITZ gel (3.2–4 hours, $p < 0.001$). This approximately 53% reduction indicates more rapid onset of drug permeation, which is particularly beneficial for topical antifungal therapy where prompt therapeutic action is required. The decreased T_{lag} can be attributed to the nanometric particle size and the permeation-enhancing properties of Poloxamer 407, which promote quicker drug partitioning into the stratum corneum lipids and faster diffusion pathway establishment.[80] The concurrent improvements in both steady-state flux (Jss) and lag time collectively demonstrate the superior permeation performance and therapeutic potential of the nanoparticle-based gel system.

The 2.45-fold enhancement ratio represents a direct functional consequence of the balanced formulation design, which provides sustained release at the application site while facilitating enhanced skin penetration. This synergistic transdermal enhancement arises from pH-dependent release aligned with the acidic skin surface (pH 4.5–5.5), resulting in

Table 5 Permeation Parameters of ITZ from Plain Gel and F2 Nanoparticle-Loaded Gel (Mean ± SD, N = 3)

Parameter	Plain ITZ Gel	F2 Nanoparticle Gel	p-value	Significance
Q_{24} (µg/cm^2)	75.35 ± 1.35	173.29 ± 3.12	<0.001	***
Jss (µg/cm^2/h)	2.58 ± 0.08	6.32 ± 0.15	<0.001	***
T_{lag} (h)	3.2 ± 0.4	1.5 ± 0.2	<0.001	***
Enhancement Ratio (ER)	1 (Reference)	2.45	—	—

Note: Cumulative amount permeated per unit area in 24 hours; Jss: Steady-state flux; Data are presented as mean ± SD (n=3). Statistical significance was determined using an unpaired, two-tailed Student's *t*-test. ***$p < 0.001$ indicates a statistically significant difference compared to the plain ITZ gel.
Abbreviations: ER, Enhancement Ratio; T_{lag}, lag time.

https://doi.org/10.2147/IJN.S560741

optimized lipophilic ITZ delivery into the stratum corneum. In parallel, Poloxamer 407 modulates stratum corneum lipids and increases permeability. The combined effects of interfacial hydration, polymer plasticization, and permeation enhancement in the PCL-Poloxamer 407 carbopol gel matrix confirm this cooperative effect. Our results indicate a two-phase reservoir-mediated mechanism governing the transdermal transport process. In the first phase, the nanoscale dimensions (~154 nm) and lipophilic PCL matrix facilitate efficient nanoparticle partitioning into the lipid-rich domains of the stratum corneum and upper epidermis,[81] leading to formation of a localized cutaneous drug reservoir that serves as a temporary depot immediately after application. In the second phase, this retained drug fraction acts as a sustained-release source, gradually liberating ITZ that diffuses through the viable epidermis and dermis. The released drug subsequently permeates into the dermal microvasculature, resulting in measurable systemic input. This interpretation is quantitatively supported by the ex vivo permeation data, which show a 2.3-fold increase in cumulative permeation (Q_{24}) and a >2.4-fold enhancement in steady-state flux (Jss) for the optimized F2 formulation in carbopol gel compared with the plain gel. These findings confirm that the skin-associated reservoir does not trap the drug but rather maintains a continuous release gradient that sustains transdermal absorption over extended periods. Essentially, the system utilizes the skin not merely as a barrier but as a biocompatible, controllable depot that modulates and prolongs drug input into systemic circulation. This depot-based release strategy minimizes plasma concentration fluctuations and offers a pharmacokinetic advantage over conventional oral ITZ, which is limited by poor solubility and variable bioavailability.[82] Therefore, the observed high skin retention represents an integral component of the transdermal design, reflecting a rational and efficient approach to achieving sustained systemic delivery.

Skin Irritation Test

The skin biocompatibility of gel loaded with ITZ has been assessed in healthy adult New Zealand white rabbits according to OECD Guideline 404.[32] Observation was carried out 24, 48 and 72 hours after application to evaluate the signs of erythema and oedema using the Draize scoring system (Table 6). The nanoparticle-loaded gel sample demonstrated good compatibility with the skin and showed no signs of erythema or oedema at any time point (24 hours, 48 hours and 72 hours) in all test animals Table 6. Conversely, the positive control group treated with 0.8% sodium lauryl sulphate (SLS) consistently showed moderate to severe erythema and mild oedema with a primary inflammatory index (PII=0), which classified it as an irritant (Figure 11).[83,84] The excellent biocompatibility of the nanoparticle-loaded gel is due to the presence of PCL nanoparticles combined with eucalyptus oil, known for its anti-inflammatory, thus preserving skin

Table 6 Skin Irritation Scores at 24 h, 48 h and 72 h in New Zealand White Rabbits

Group	Animal No.	Erythema (24 h)	Edema (24 h)	Total (24 h)	Erythema (48 h)	Edema (48 h)	Total (48 h)	Erythema (72 h)	Edema (72 h)	Total (72 h)
Test Group	1	0	0	0	0	0	0	0	0	0
	2	0	0	0	0	0	0	0	0	0
	3	0	0	0	0	0	0	0	0	0
Mean ± SD		0.00 ± 0.00	0.00 ± 0.00	0.00 ± 0.00	0.00 ± 0.00	0.00 ± 0.00	0.00 ± 0.00	0.00 ± 0.00	0.00 ± 0.00	0.00 ± 0.00
Positive Control	4	2	1	3	2	1	3	2	1	3
	5	3	1	4	2	1	3	2	1	3
	6	3	2	5	2	1	3	2	1	3
Mean ± SD		2.67 ± 0.58	1.33 ± 0.58	4.00 ± 1.00	2.00 ± 0.00	1.00 ± 0.00	3.00 ± 0.00	2.00 ± 0.00	1.00 ± 0.00	3.00 ± 0.00
Negative Control	7	0	0	0	0	0	0	0	0	0
	8	0	0	0	0	0	0	0	0	0
	9	0	0	0	0	0	0	0	0	0
Mean ± SD		0.00 ± 0.00	0.00 ± 0.00	0.00 ± 0.00	0.00 ± 0.00	0.00 ± 0.00	0.00 ± 0.00	0.00 ± 0.00	0.00 ± 0.00	0.00 ± 0.00

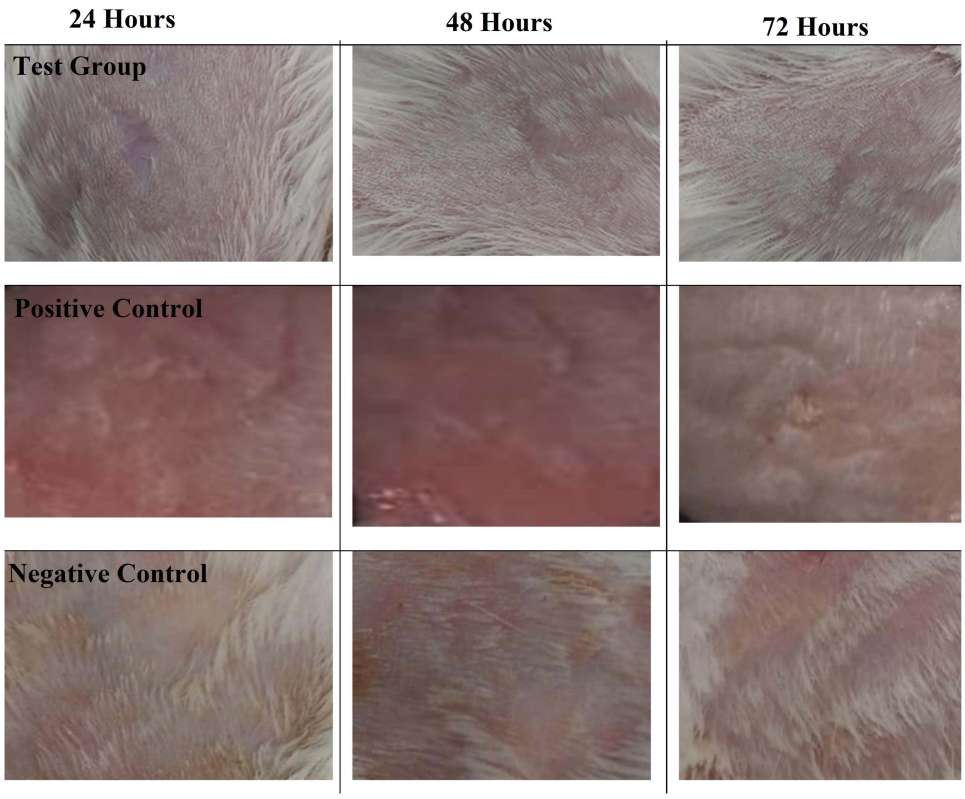

Figure 11 Comparison of Skin Irritation Responses Over 24, 48 and 72 Hours across Test Group, Positive Control, and Negative Control Groups.

integrity and preventing irritation. The results suggest that the ITZ-loaded gel is safe for skin application with therapeutic benefits without compromising cutaneous tolerance and can therefore become a candidate for clinical use.

Stability

Stability tests were performed to assess the physical integrity, pH consistency and rheological behaviour of the F2 gel formulation for three months under the storage conditions recommended in the ICH Q1A(R2) guidelines. The gel formulation was stored under three temperature conditions: refrigerated (4 ± 1°C), ambient (25 ± 2°C), and accelerated (40 ± 2°C/75 ± 5% RH) as indicated in Table 7. The optimized F2 formulation was evaluated at 1, 2, and 3 months for visual characteristics, pH, and viscosity. The optimized F2 formulation was physically stable throughout the study. No changes in appearance, such as phase separation, precipitation or colouring, were observed under any of the test conditions, which confirmed the physical integrity of the formulation. The initial pH of F2 was 6.48 ± 0.02. The pH

Table 7 Stability Parameters of F2 Gel Formulation Stored Under ICH Conditions Over 3 months

Time (months)	Storage Temp	Appearance	pH ± SD	Viscosity (cP) ± SD	% Viscosity Change
1	4°C	Clear, homogeneous	6.46 ± 0.01	13,360 ± 125	−0.67%
1	25°C	Clear, homogeneous	6.43 ± 0.02	13,220 ± 150	−1.71%
1	40°C	Clear, homogeneous	6.38 ± 0.03	12,890 ± 170	−4.16%
2	4°C	Clear, homogeneous	6.44 ± 0.02	13,290 ± 120	−1.19%
2	25°C	Clear, homogeneous	6.39 ± 0.02	13,150 ± 135	−2.23%
2	40°C	Clear, homogeneous	6.29 ± 0.04	12,650 ± 160	−5.95%
3	4°C	Clear, homogeneous	6.42 ± 0.02	13,190 ± 110	−1.93%
3	25°C	Clear, homogeneous	6.34 ± 0.03	12,970 ± 145	−3.56%
3	40°C	Clear, homogeneous	6.22 ± 0.03	12,380 ± 130	−7.95%

https://doi.org/10.2147/IJN.S560741

ranged within the acceptable range of ±0.5 units in all storage conditions and time points. In accelerated conditions (40°C), a slight decrease in pH was observed, reaching 6.22 ± 0.03 over three months, but still within the stability limits. The change in viscosity at refrigerated and ambient temperatures was <5%. At 40°C, the viscosity decreased gradually, with a maximum decrease of approximately 7.95% after three months. These changes remained within the pre-specified margin of error of ±10%. Moreover, the formulation retained its shear-thinning behaviour, which indicates structural integrity of the gel matrix. The decrease in viscosity at higher temperatures is attributable to the relaxation of the polymer or to the decreased hydrogen bonding interactions due to thermal stress.[85,86] However, the F2 formulation has maintained its rheological and physicochemical properties, which support its suitability for long-term storage.

Conclusion

This study successfully developed a PCL-based nanoparticle system for enhanced transdermal delivery of ITZ. The optimized formulation demonstrated excellent drug loading capacity (88.4%), ideal particle characteristics (154.6 nm) for skin penetration, and sustained release properties. The nanoparticle-loaded gel showed remarkable transdermal permeation enhancement (a 2.45-fold increase) compared to conventional formulations, along with excellent stability and a proven safety profile. While these results demonstrate substantial promise for transdermal antifungal delivery, we acknowledge the need for future in vivo studies to validate therapeutic efficacy in appropriate infection models. This nanotechnology platform effectively overcomes the solubility and permeability challenges of ITZ, representing a significant advancement in transdermal drug delivery systems for poorly soluble antifungal agents.

Data Sharing Statement

The authors confirm that the data supporting the findings of this study are available within the article.

Ethical Approval Statement

This study received ethical approval from the Research Ethics Committee of the Faculty of Pharmacy, Capital University of Science and Technology, Islamabad (Approval No. REC/FoP/F2024/02). All experimental procedures were conducted following institutional ethical guidelines.

Acknowledgment

Authors sincerely thank the support from the Post-Doctoral Research Start-Up Fund of Lishui People's Hospital, Grant No. 2024bsh002, Lishui, Zhejiang, China.

Author Contributions

All authors made a significant contribution to the work reported, whether that is in the conception, study design, execution, acquisition of data, analysis and interpretation, or in all these areas; took part in drafting, revising or critically reviewing the article; gave final approval of the version to be published; have agreed on the journal to which the article has been submitted; and agree to be accountable for all aspects of the work.

Disclosure

The authors declare no conflicts of interest.

References

1. Lee E-A, Balakrishnan P, Song C-K, et al. Microemulsion-based hydrogel formulation of itraconazole for topical delivery. *J Pharm Invest*. 2010;40(5):305–311. doi:10.4333/KPS.2010.40.5.305
2. Yadollahi R, Vasilev K, Simovic S, Chen H. Nanosuspension technologies for delivery of poorly soluble drugs. *J Nanomater*. 2015;2015(1):216375. doi:10.1155/2015/216375
3. Amidon GL, Lennernäs H, Shah VP, et al. A theoretical basis for a biopharmaceutic drug classification: the correlation of in vitro drug product dissolution and in vivo bioavailability. *Pharm Res*. 1995;12(3):413–420. doi:10.1023/A:1016212804288
4. Zeb A, Arif ST, Malik M, et al. Potential of nanoparticulate carriers for improved drug delivery via skin. *J Pharm Invest*. 2019;49(5):485–517. doi:10.1007/s40005-018-00418-8

5. Patel Tejas B, Tushar RP, Suhagia B. Preparation, characterization, and optimization of microemulsion for topical delivery of itraconazole. *J Drug Delivery Ther*. 2018;8(2):136–145.
6. Stella VJ, Rao VM, Zannou EA, et al. Mechanisms of drug release from cyclodextrin complexes. *Adv Drug Delivery Rev*. 1999;36(1):3–16. doi:10.1016/S0169-409X(98)00052-0
7. Łukasiewicz S, Mikołajczyk A, Błasiak E, et al. Polycaprolactone nanoparticles as promising candidates for nanocarriers in novel nanomedicines. *Pharmaceutics*. 2021;13(2):191. doi:10.3390/pharmaceutics13020191
8. Dumortier G, Grossiord JL, Agnely F, et al. A review of poloxamer 407 pharmaceutical and pharmacological characteristics. *Pharm Res*. 2006;23 (12):2709–2728. doi:10.1007/s11095-006-9104-4
9. Nguyen -T-T-L, Duong V-A, Maeng H-J. Pharmaceutical formulations with P-glycoprotein inhibitory effect as promising approaches for enhancing oral drug absorption and bioavailability. *Pharmaceutics*. 2021;13(7):1103. doi:10.3390/pharmaceutics13071103
10. Kolluru LP, Chandran T, Shastri PN, et al. Development and evaluation of polycaprolactone based docetaxel nanoparticle formulation for targeted breast cancer therapy. *J Nanopart Res*. 2020;22:1–14. doi:10.1007/s11051-020-05096-y
11. Ubaid M, Ilyas S, Mir S, et al. Formulation and in vitro evaluation of carbopol 934-based modified clotrimazole gel for topical application. *Anais da Academia Brasileira de Ciências*. 2016;88(4):2303–2317. doi:10.1590/0001-3765201620160162
12. Kuddushi M, Kanike C, Xu BB, et al. Recent advances in nanoprecipitation: from mechanistic insights to applications in nanomaterial synthesis. *Soft Matter*. 2025;21(15):2759–2781. doi:10.1039/D5SM00006H
13. Saqib M, Ali bhatti AS, Ahmad NM, et al. Amphotericin b loaded polymeric nanoparticles for treatment of leishmania infections. *Nanomaterials*. 2020;10(6):1152. doi:10.3390/nano10061152
14. Abriata JP, Turatti RC, Luiz MT, et al. Development, characterization and biological in vitro assays of paclitaxel-loaded PCL polymeric nanoparticles. *Mater Sci Eng C*. 2019;96:347–355.
15. Stancu AI, Oprea E, Dițu LM, et al. Development, optimization, and evaluation of new gel formulations with cyclodextrin complexes and volatile oils with antimicrobial activity. *Gels*. 2024;10(10):645. doi:10.3390/gels10100645
16. Patil AS, Chougale SS, Kokatanr U, et al. Formulation and evaluation of itraconazole-loaded nanoemulgel for efficient topical delivery to treat fungal infections. *Therapeutic Delivery*. 2024;15(3):165–179. doi:10.4155/tde-2023-0062
17. Soundarya T, Jayachandran M, Maiyalagan T, et al. A novel one-pot synthesis strategy for β-Mn2V2O7 nanorods synthesized via 1-(3, 6-dioxa heptane) 3-methyl imidazolium methane sulfonate-assisted hydrothermal route for sustainable and on-demand advanced supercapacitor electrodes and as negative electrode materials for Li-ion batteries. *J Energy Storage*. 2024;85:111076.
18. Parikh S, Patel AD, Dave JB, et al. Development and validation of UV spectrophotometric method for estimation of Itraconazole bulk drug and pharmaceutical formulation. *Inter J Drug Develop Res*. 2011;3:324–328.
19. Hamishehkar H, Emami S, Lamei B, et al. Evaluation of solubility and dissolution profile of itraconazole after cogrinding with various hydrophilic carriers. *J Drug Delivery Sci Technol*. 2014;24(6):653–658. doi:10.1016/S1773-2247(14)50132-3
20. Botros SR, Hussein AK, Mansour HF. A novel nanoemulsion intermediate gel as a promising approach for delivery of itraconazole: design, in vitro and ex vivo appraisal. *AAPS Pharm Sci Tech*. 2020;21(7):1–13. doi:10.1208/s12249-020-01830-w
21. Damodharan N, Damodharan N. Mathematical modelling of dissolution kinetics in dosage forms. *Res J Pharm Technol*. 2020;13(3):1339–1345. doi:10.5958/0974-360X.2020.00247.4
22. Ertugral-Samgar EG, Ozmen AM, Gok O. Thermo-responsive hydrogels encapsulating targeted core–shell nanoparticles as injectable drug delivery systems. *Pharmaceutics*. 2023;15(9):2358. doi:10.3390/pharmaceutics15092358
23. Danafar H, Davaran S, Rostamizadeh K, et al. Biodegradable m-PEG/PCL core-shell micelles: preparation and characterization as a sustained release formulation for curcumin. *Adv Pharm Bull*. 2014;4(Suppl 2):501. doi:10.5681/apb.2014.074
24. El-Housiny S, Shams Eldeen MA, El-Attar YA, et al. Fluconazole-loaded solid lipid nanoparticles topical gel for treatment of pityriasis versicolor: formulation and clinical study. *Drug Delivery*. 2018;25(1):78–90. doi:10.1080/10717544.2017.1413444
25. Ho HN, Le TG, Dao TTT, et al. Development of itraconazole-loaded polymeric nanoparticle dermal gel for enhanced antifungal efficacy. *J Nanomater*. 2020;2020(1):8894541. doi:10.1155/2020/8894541
26. Hazer B, Modjinou T, Langlois V, et al. Free radical polymerization of dimethyl amino ethyl methacrylate initiated by poly (3-hydroxybutyrate-co -3-hydroxyhexanoate) macroazo initiator: thermal and physicochemical characterization. *J Polym Environ*. 2023;31(8):3688–3699. doi:10.1007/s10924-023-02857-3
27. Alhowyan AA, Altamimi MA, Kalam MA, et al. Antifungal efficacy of Itraconazole loaded PLGA-nanoparticles stabilized by vitamin-E TPGS: in vitro and ex vivo studies. *J Microbiol Methods*. 2019;161:87–95. doi:10.1016/j.mimet.2019.01.020
28. Badawi AA, El-Nabarawi MA, El-Setouhy DA, et al. Formulation and stability testing of itraconazole crystalline nanoparticles. *AAPS Pharm Sci Tech*. 2011;12(3):811–820. doi:10.1208/s12249-011-9651-9
29. Desai KGH. Enhanced skin permeation of rofecoxib using topical microemulsion gel. *Drug Dev Res*. 2004;63(1):33–40. doi:10.1002/ddr.10386
30. Kumar M, Sharma A, Mahmood S, et al. Franz diffusion cell and its implication in skin permeation studies. *J Dispers Sci Technol*. 2024;45 (5):943–956. doi:10.1080/01932691.2023.2188923
31. Soundarya G, Rao PV, Chandrika C, et al. Method development and analytical method validation of itraconazole by using uv-visible spectrophotometry. *Indo Ame j pharmaceusci*. 2016;3(5):487–491.
32. Wilhelm K-P, Maibach HI. *OECD Guidelines for Testing of Chemicals, in Dermatotoxicology*. CRC press; 2012:509–511.
33. Care, I.o.L.A.R.C.o. and U.o.L. Animals. *Guide for the Care and Use of Laboratory Animals*. National: US Department of Health and Human Services, Public Health Service; 1986.
34. Friedman N, Merims S, Elia J, et al. Ex-vivo skin permeability tests of nanoparticles for microscopy imaging. *Bio-Protocol*. 2022;12(7):e4375–e4375. doi:10.21769/BioProtoc.4375
35. OECD. *OECD Guidelines for the Testing of Chemicals*. Oecd; 1994.
36. Zothanpuii F, Rajesh R, Selvakumar K. A review on stability testing guidelines of pharmaceutical products. *Asian J Pharm Clin Res*. 2020;13 (10):3–9.
37. Gajra B, Dalwadi C, Patel R. Formulation and optimization of itraconazole polymeric lipid hybrid nanoparticles (Lipomer) using box behnken design. *DARU J Pharma Sci*. 2015;23(1):1–15. doi:10.1186/s40199-014-0087-0

38. Wadile KA, Ige PP, Sonawane RO. Preparation of itraconazole nanoparticles and its topical nanogel: physicochemical properties and stability studies. *Int J Pharm Sci Dev Res*. 2019;5(1):001–008.
39. Rana SS, Bhatt S, Kumar M, et al. Design and optimization of itraconazole loaded SLN for intranasal administration using central composite design. *Nanosci Nanotechnol Asia*. 2020;10(6):884–891. doi:10.2174/2210681209666191111113112
40. Ullah F, Iqbal Z, Khan A, et al. Formulation development and characterization of pH responsive polymeric nano-pharmaceuticals for targeted delivery of anti-cancer drug (methotrexate). *Front Pharmacol*. 2022;13:911771. doi:10.3389/fphar.2022.911771
41. Lee KH, Khan FN, Cosby L, et al. Polymer concentration maximizes encapsulation efficiency in electrohydrodynamic mixing nanoprecipitation. *Front Nanotechnol*. 2021;3:719710. doi:10.3389/fnano.2021.719710
42. Ansari M. Factors affecting preparation and properties of nanoparticles by nanoprecipitation method. *Indo Ame J Pharmaceu Sci*. 2017;4 (12):4854–4858.
43. Paramashivaiah B, Rajashekhar C Studies on effect of various surfactants on stable dispersion of graphene nanoparticles in Simarouba biodiesel. In: IOP Conference Series: Materials Science and Engineering; Bengaluru, India;: Vol. 149. ICAMA–2016.
44. Thapa RK, Cazzador F, Grønlien KG, et al. *Effect of curcumin and cosolvents on the micellization of Pluronic F127 in aqueous solution*. Colloids and Surfaces B. *Biointerfaces*. 2020;195:111250. doi:10.1016/j.colsurfb.2020.111250
45. Heydarinasab H, Haddadi-ASL V, Ahmadi H. A comprehensive review of nano-deposition methods for the preparation of nano-carriers: polymers, drugs, and drug release models. *Austin Med Sci*. 2024;9(1).
46. Patravale VB, Desai PP Topical nanointerventions for therapeutic and cosmeceutical applications. In: Domb A Khan W, editors. Focal Controlled Drug Delivery. Springer; 2014pp. 535–560.
47. Turan CU, Metin A, Guvenilir Y. Controlled release of tetracycline hydrochloride from poly (ω-pentadecalactone-co-ε-caprolactone)/gelatin nanofibers. *Eur J Pharm Biopharm*. 2021;162:59–69. doi:10.1016/j.ejpb.2021.02.009
48. Altun E, Yuca E, Ekren N, et al. Kinetic release studies of antibiotic patches for local transdermal delivery. *Pharmaceutics*. 2021;13(5):613. doi:10.3390/pharmaceutics13050613
49. Ciftci F, Özarslan AC. Fabrication of polycaprolactone-chitosan/curcumin polymer composite fibers and evaluation of their in vitro release kinetic behavior and antibacterial-antifungal activity. *J Sol Gel Sci Techn*. 2024;109(1):192–203. doi:10.1007/s10971-023-06264-x
50. Abdeltawab H, Svirskis D, Sharma M. Formulation strategies to modulate drug release from poloxamer based in-situ gelling systems. *Expert Opin Drug Delivery*. 2020;17.
51. Ekenna IC, Abali SO. Comparison of the use of kinetic model plots and DD solver software to evaluate the drug release from griseofulvin tablets. *J Drug Delivery Ther*. 2022;12(2–S):5–13. doi:10.22270/jddt.v12i2-S.5402
52. Nasr FH, Khoee S, Dehghan MM, et al. Preparation and evaluation of contact lenses embedded with polycaprolactone-based nanoparticles for ocular drug delivery. *Biomacromolecules*. 2016;17(2):485–495. doi:10.1021/acs.biomac.5b01387
53. Dash TK, Konkimalla VB. Poly-ϵ-caprolactone based formulations for drug delivery and tissue engineering: a review. *J Control Release*. 2012;158 (1):15–33. doi:10.1016/j.jconrel.2011.09.064
54. Badri W, Miladi K, Nazari QA, et al. Effect of process and formulation parameters on polycaprolactone nanoparticles prepared by solvent displacement. *Colloids Surf A*. 2017;516:238–244. doi:10.1016/j.colsurfa.2016.12.029
55. Zhang Z, Tsai P-C, Ramezanli T, et al. Polymeric nanoparticles-based topical delivery systems for the treatment of dermatological diseases. *Wiley Interdiscip Rev Nanomed Nanobiotechnol*. 2013;5(3):205–218. doi:10.1002/wnan.1211
56. Danaei M, Dehghankhold M, Ataei S, et al. Impact of particle size and polydispersity index on the clinical applications of lipidic nanocarrier systems. *Pharmaceutics*. 2018;10(2):57. doi:10.3390/pharmaceutics10020057
57. Honary S, Zahir F. Effect of zeta potential on the properties of nano-drug delivery systems-a review (Part 2). *Trop J Pharm Res*. 2013;12 (2):265–273.
58. Wan Y, Gan Z, Li Z. Effects of the surface charge on the stability of PEG-b-PCL micelles: simulation of the interactions between charged micelles and plasma components. *Polym Chem*. 2014;5(5):1720–1727. doi:10.1039/C3PY01281F
59. Cortés H, Hernández-Parra H, Bernal-Chávez SA, et al. Non-ionic surfactants for stabilization of polymeric nanoparticles for biomedical uses. *Materials*. 2021;14(12):3197. doi:10.3390/ma14123197
60. Kumar SS. Formulation and characterization of noscapine-loaded polycaprolactone nanoparticles. *Asian J Pharmaceu*. 2019;13(01).
61. Lemaire V, Belair J, Hildgen P. Structural modeling of drug release from biodegradable porous matrices based on a combined diffusion/erosion process. *Int J Pharm*. 2003;258(1–2):95–107. doi:10.1016/S0378-5173(03)00165-0
62. Javaid S, Ahmad NM, Mahmood A, et al. Cefotaxime loaded polycaprolactone based polymeric nanoparticles with antifouling properties for in-vitro drug release applications. *Polymers*. 2021;13(13):2180. doi:10.3390/polym13132180
63. Kujawski J, Czaja K, Jodłowska-Siewert E, et al. Structural and spectroscopic properties of itraconazole and ketoconazole–Experimental and theoretical studies. *J Mol Struct*. 2017;1146:259–266. doi:10.1016/j.molstruc.2017.05.128
64. Elzein T, Nasser-Eddine M, Delaite C, et al. FTIR study of polycaprolactone chain organization at interfaces. *J Colloid Interface Sci*. 2004;273 (2):381–387. doi:10.1016/j.jcis.2004.02.001
65. Vyas V, Sancheti P, Karekar P, et al. Physicochemical characterization of solid dispersion systems of tadalafil with poloxamer 407. *Acta Pharm*. 2009;59(4):453–461. doi:10.2478/v10007-009-0037-4
66. Fathima N, Mamatha T, Qureshi H, et al. Drug-excipient interaction and its importance in dosage form development. *J Appl Pharm Sci*. 2011;66–71.
67. Lucena PA, Nascimento TL, Gaeti MPN, et al. In vivo vaginal fungal load reduction after treatment with itraconazole-loaded polycaprolactone-nanoparticles. *J Biomed Nanotechnol*. 2018;14(7):1347–1358. doi:10.1166/jbn.2018.2574
68. Ling X, Huang Z, Wang J, et al. Development of an itraconazole encapsulated polymeric nanoparticle platform for effective antifungal therapy. *J Mat Chem B*. 2016;4(10):1787–1796. doi:10.1039/C5TB02453F
69. Randall CS, Rocco WL, Rico P. XRD: XRD in pharmaceutical analysis: a versatile tool for problem-solving. *Am Pharm Rev*. 2010;13(6):52.
70. Kim DH, Kim Y, Tin -Y-Y, et al. Recent technologies for amorphization of poorly water-soluble drugs. *Pharmaceutics*. 2021;13(8):1318. doi:10.3390/pharmaceutics13081318
71. Karagianni A, Kachrimanis K, Nikolakakis I. Co-amorphous solid dispersions for solubility and absorption improvement of drugs: composition, preparation. *Characteriz Formul Oral Delivery Pharmaceu*. 2018;10(3).

72. Tao T, Zhao Y, Wu J, et al. Preparation and evaluation of itraconazole dihydrochloride for the solubility and dissolution rate enhancement. *Int J Pharm*. 2009;367(1–2):109–114. doi:10.1016/j.ijpharm.2008.09.034
73. Plivelic TS, Cassu SN, Do Carmo Gonçalves M, et al. Structure and morphology of poly (ε-caprolactone)/chlorinated polyethylene (PCL/PECl) blends investigated by DSC, simultaneous SAXS/WAXD, and elemental mapping by ESI-TEM. *Macromolecules*. 2007;40(2):253–264. doi:10.1021/ma061265m
74. Zhang S, Lee TW, Chow AH. Crystallization of itraconazole polymorphs from melt. *Cryst Growth Des*. 2016;16(7):3791–3801. doi:10.1021/acs.cgd.6b00342
75. Veras FF, Ritter AC, Roggia I, et al. Natamycin-loaded electrospun poly (ε-caprolactone) nanofibers as an innovative platform for antifungal applications. *SN Appl Sci*. 2020;2(6):1–14. doi:10.1007/s42452-020-2912-z
76. Shin S-C, Kim J-Y, Oh I-J. Mucoadhesive and physicochemical characterization of carbopol-poloxamer gels containing triamcinolone acetonide. *Drug Dev Ind Pharm*. 2000;26(3):307–312. doi:10.1081/DDC-100100358
77. Bala P, Jathar S, Kale S, et al. Transdermal drug delivery system (TDDS)-a multifaceted approach for drug delivery. *J Pharm Res*. 2014;8(12):1805–1835.
78. Waheed A, Ahad A, Gupta DK, et al. *Nanovesicles for the Treatment of Skin Disorders, in Applications of Nanovesicular Drug Delivery*. Elsevier; 2022:285–302.
79. Lunter D, Klang V, Eichner A, et al. Progress in topical and transdermal drug delivery research—focus on nanoformulations. *Pharmaceutics*. 2024;16(6):817. doi:10.3390/pharmaceutics16060817
80. Ghasemiyeh P, Mohammadi-Samani S. Potential of nanoparticles as permeation enhancers and targeted delivery options for skin: advantages and disadvantages. *Drug Des Devel Ther*. 2020;Volume 14:3271–3289. doi:10.2147/DDDT.S264648
81. Sirisha V, Sailaja A. Review on recent approaches in transdermal drug delivery system. *J Nurs Patient Health Care*. 2018;1(1):103.
82. Kim H, Jung S, Yeo S, et al. Characteristics of skin deposition of itraconazole solubilized in cream formulation. *Pharmaceutics*. 2019;11(4):195. doi:10.3390/pharmaceutics11040195
83. Charmeau-Genevois C, Sarang S, Perea M, et al. A simplified index to quantify the irritation/corrosion potential of chemicals–Part I: skin. *Regul Toxicol Pharmacol*. 2021;123:104922. doi:10.1016/j.yrtph.2021.104922
84. Charmeau-Genevois C, Sarang S, Perea M, et al. A simplified index to quantify the irritation/corrosion potential of chemicals–Part II: eye. *Regul Toxicol Pharmacol*. 2021;123:104935. doi:10.1016/j.yrtph.2021.104935
85. Tayel SA, El-Nabarawi MA, Tadros MI, et al. Positively charged polymeric nanoparticle reservoirs of terbinafine hydrochloride: preclinical implications for controlled drug delivery in the aqueous humor of rabbits. *AAPS Pharm Sci Tech*. 2013;14(2):782–793. doi:10.1208/s12249-013-9964-y
86. Sakhi M, Khan A, Khan I, et al. Effect of polymeric stabilizers on the size and stability of PLGA paclitaxel nanoparticles. *Saudi Pharm J*. 2023;31(9):101697. doi:10.1016/j.jsps.2023.101697